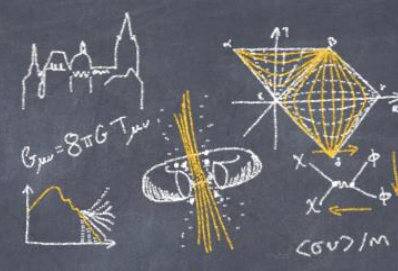


COSMO'19

RWTH Aachen University  
2-6 September, Germany



UNIVERSITY OF  
OXFORD

# TOMOGRAPHIC MEASUREMENT OF THE COSMIC GAS PRESSURE

**NICK KOUKOUFILIPPAS**

DPhil student, University of Oxford  
Nick.Koukoufilippas@physics.ox.ac.uk

*also: David Alonso (Oxford), Maciej Bilicki (Polish Academy of Sciences), John Peacock (Edinburgh)*



motivation

analysis

results

conclusions

**motivation**

analysis

results

conclusions



motivation

**analysis**

results

conclusions

motivation

analysis

**results**

conclusions



motivation

analysis

results

**conclusions**



motivation

analysis

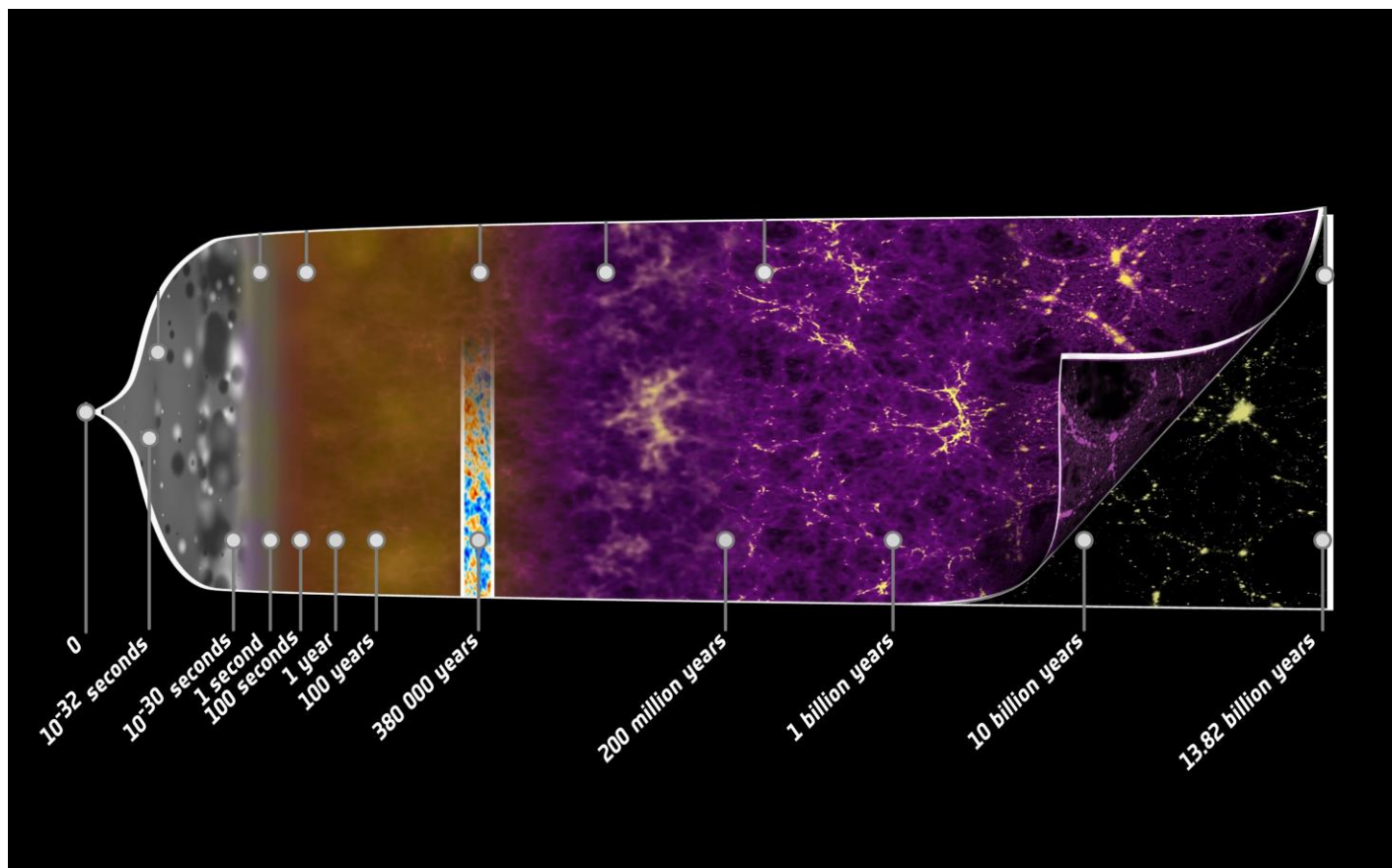
results

conclusions

# Gas Pressure? huh?

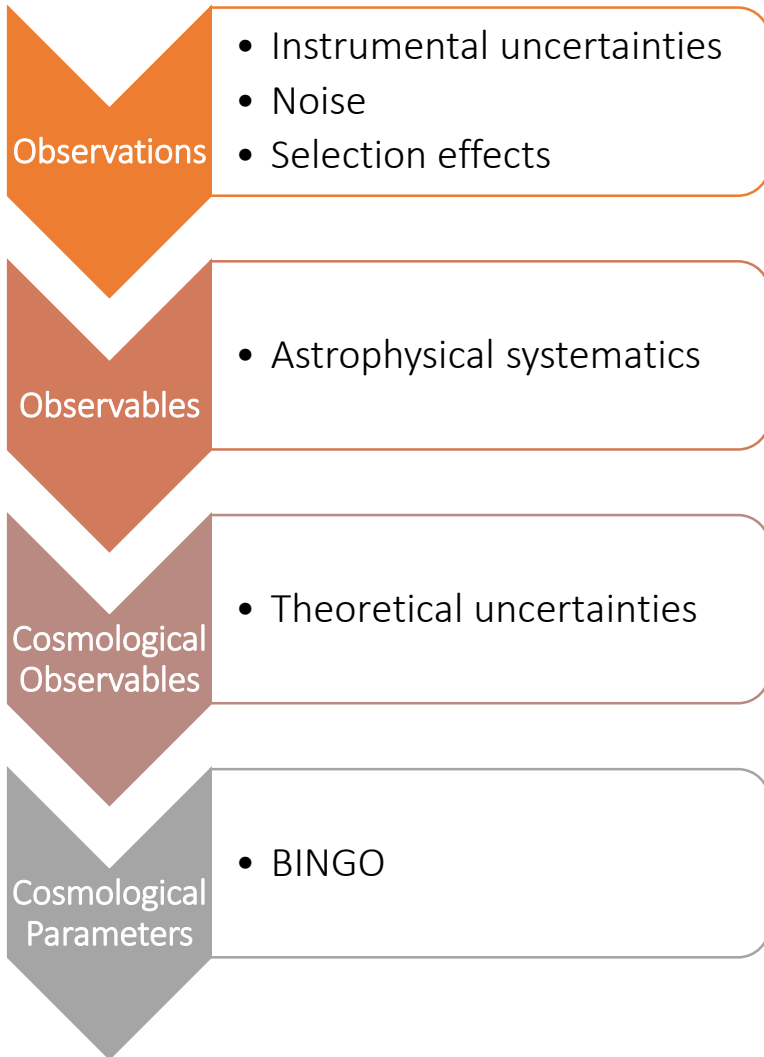
# Gas Pressure? huh?

- ✓ high-precision cosmology
- ✓ probe fundamental physics

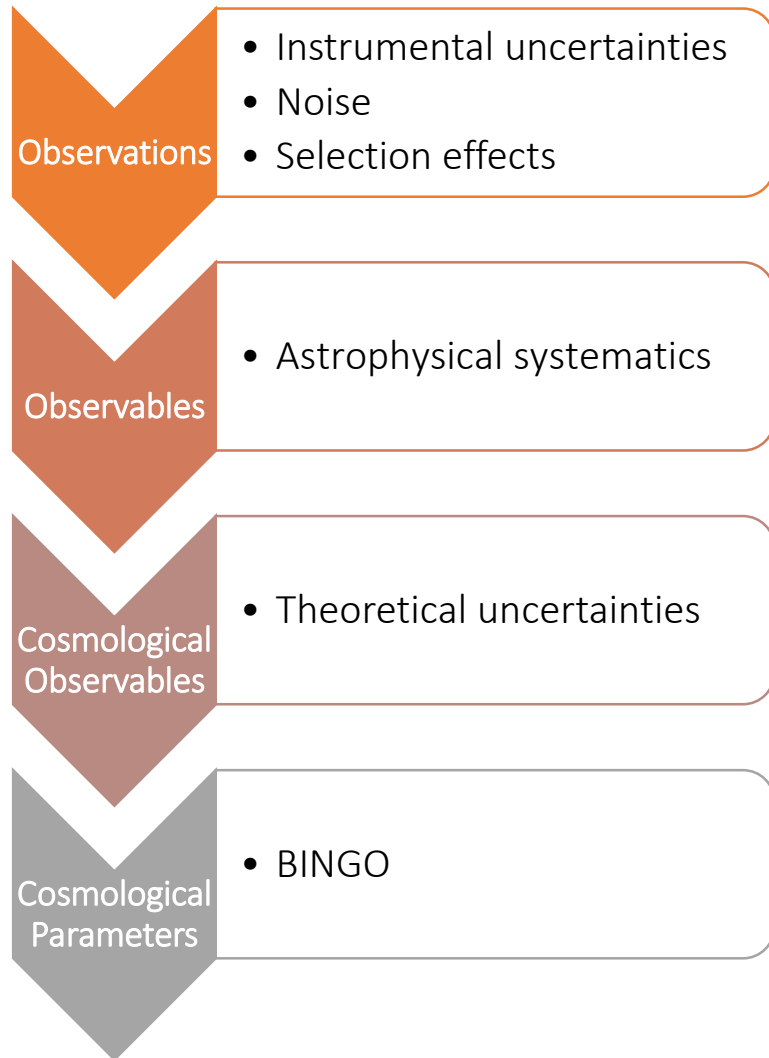


# Gas Pressure? huh?

# Gas Pressure? huh?

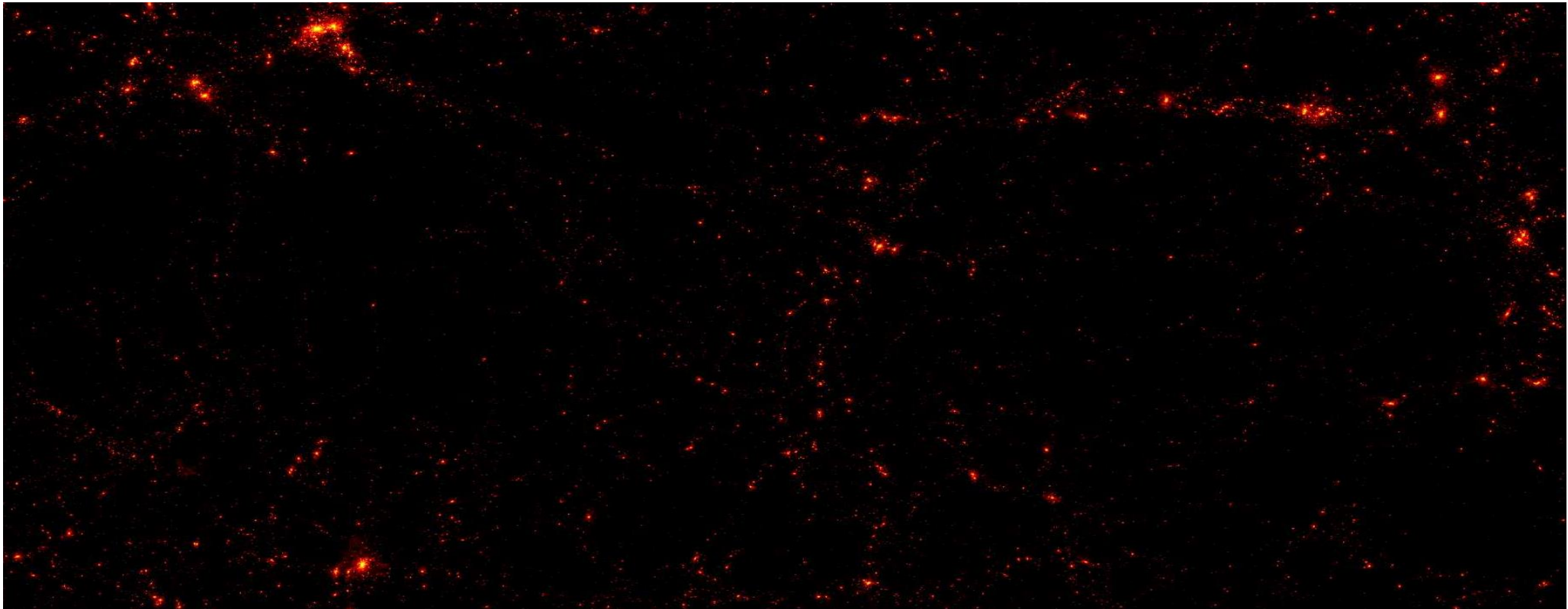


# Gas Pressure? huh?

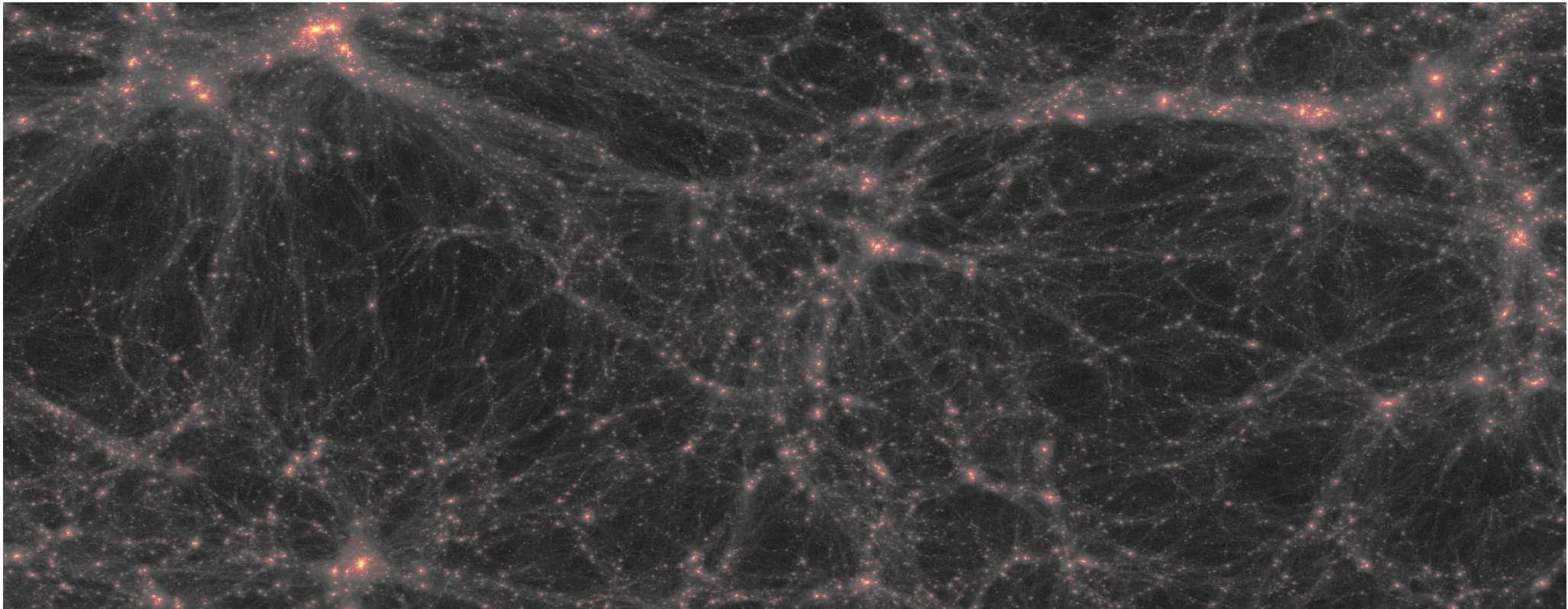


**X** we don't know the **small-scale hydrodynamics**

# What we don't understand very well

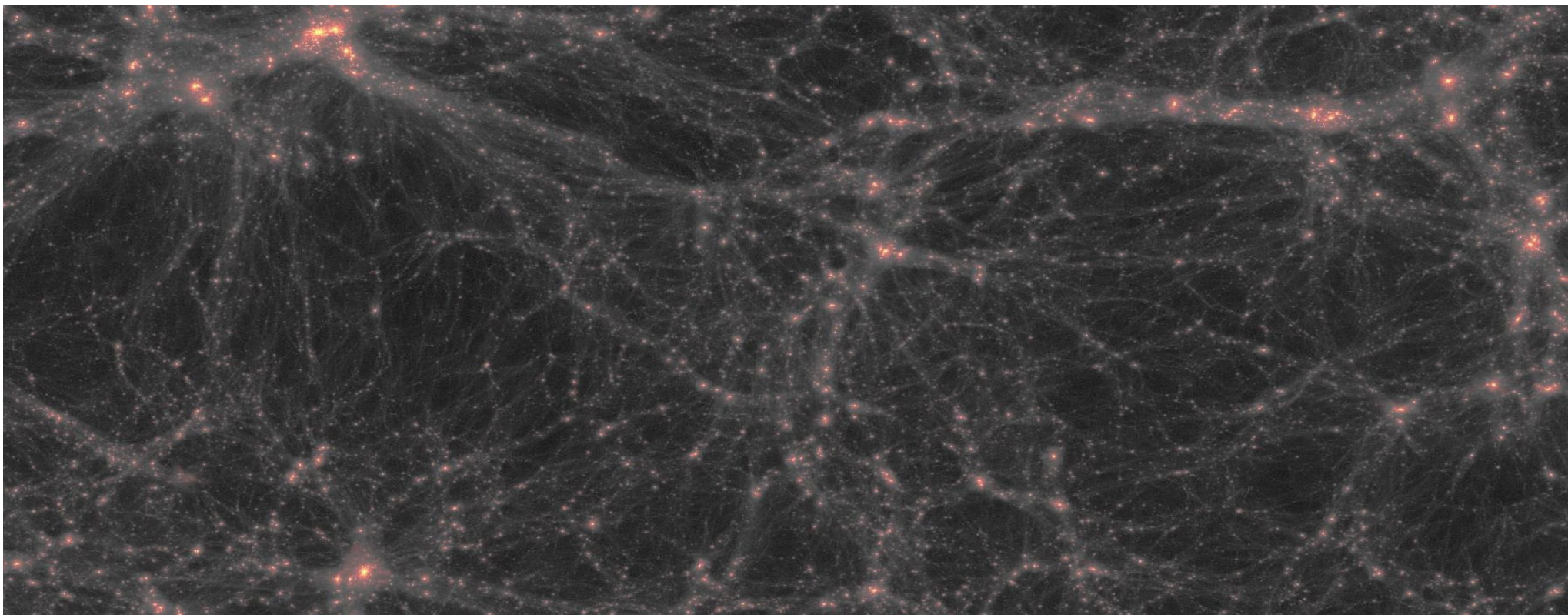


# What we don't understand very well



# What we don't understand very well

Clustering of galaxies	Galaxy-DM connection
Cluster number counts	Mass-Observable relation
Cosmic shear	Baryonic feedback / Intrinsic alignments
CMB	Small-scale astrophysical foregrounds



# What we don't understand very well



Clustering of galaxies

Galaxy-DM connection

Cluster number counts

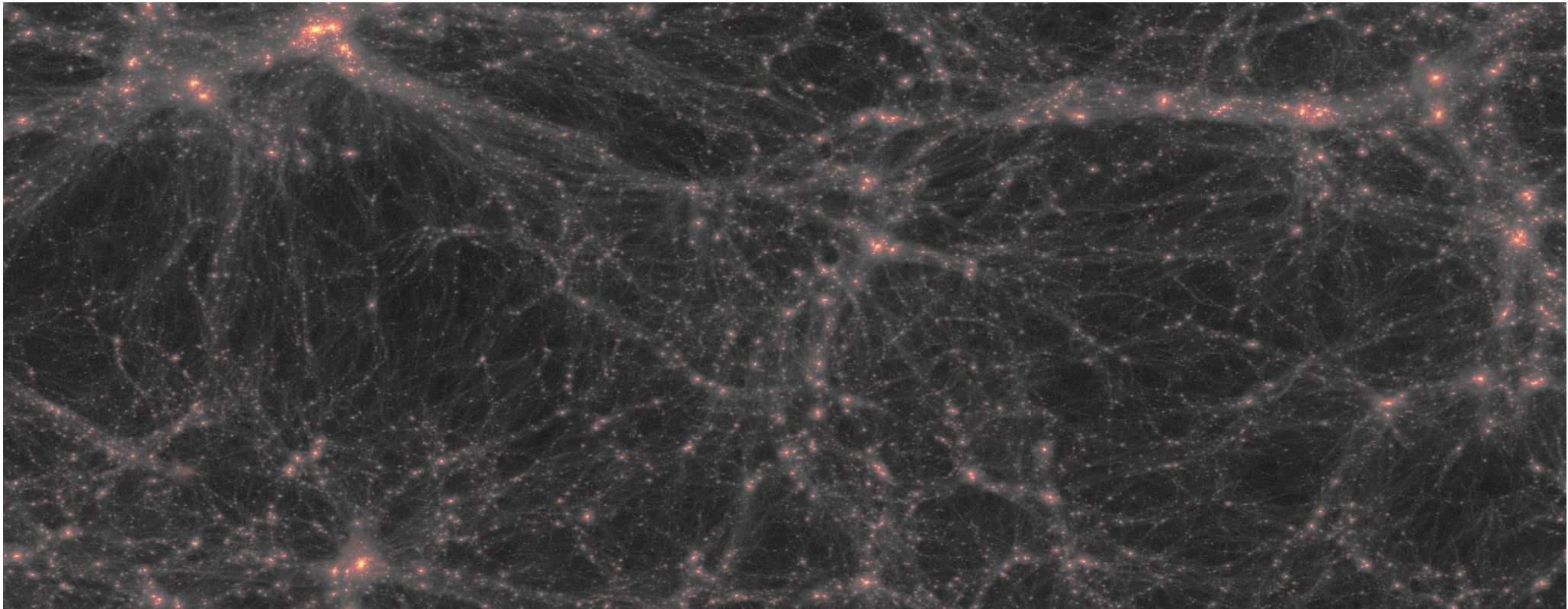
Mass-Observable relation

Cosmic shear

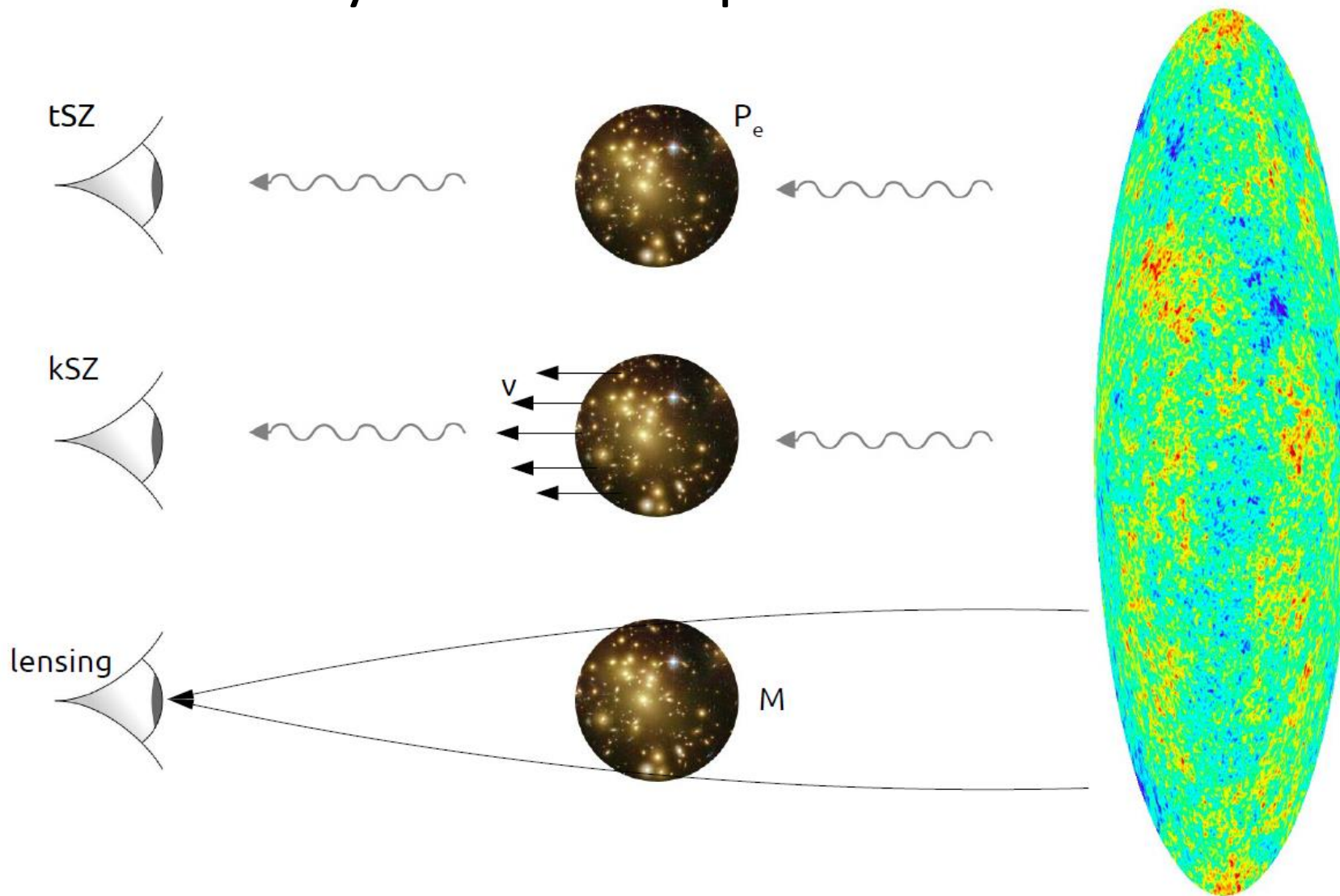
Baryonic feedback / Intrinsic alignments

CMB

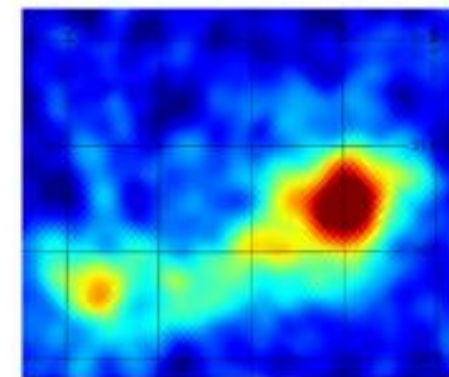
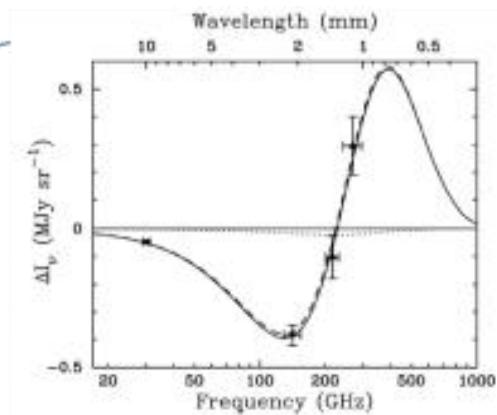
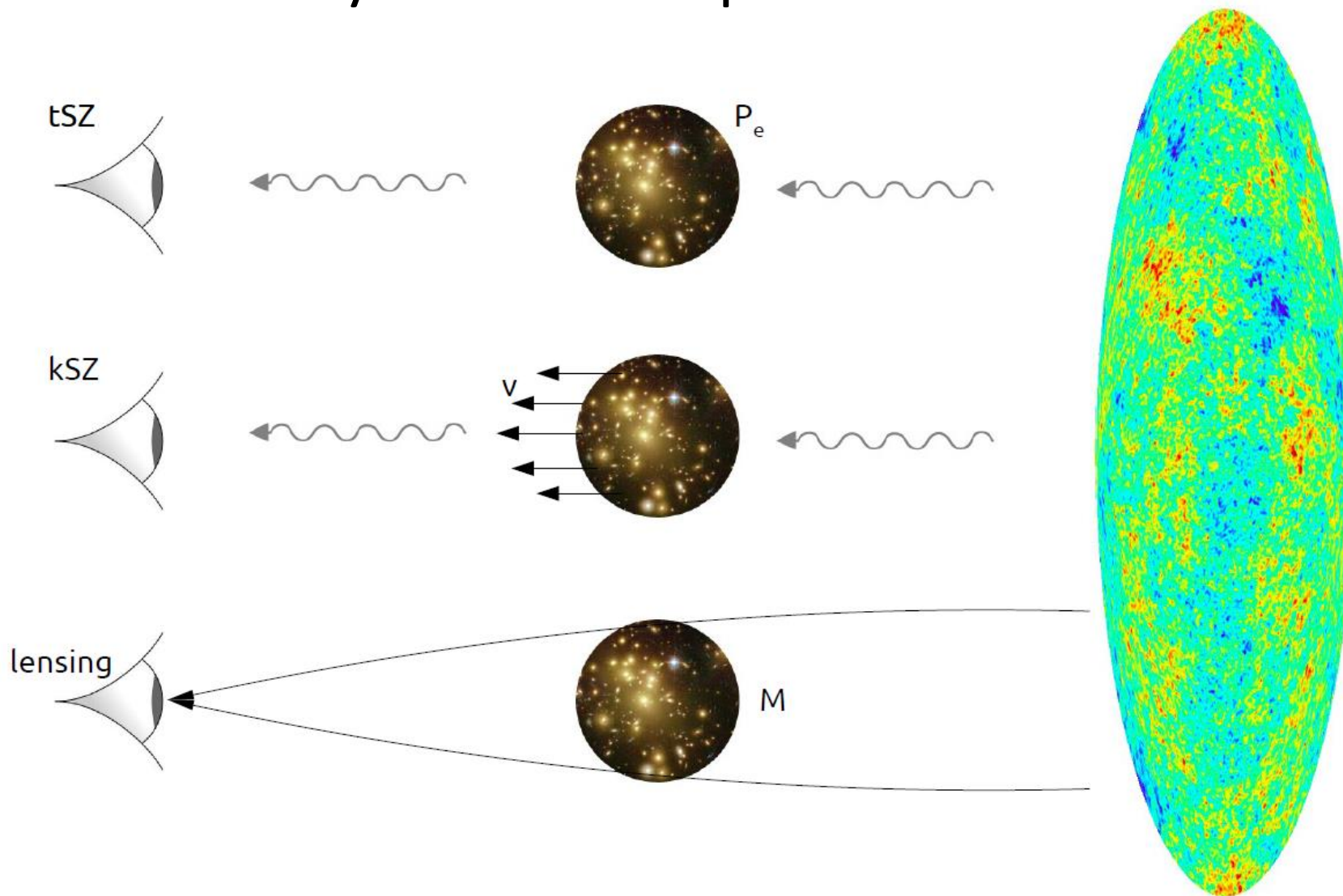
Small-scale astrophysical foregrounds



# Secondary anisotropies of the CMB

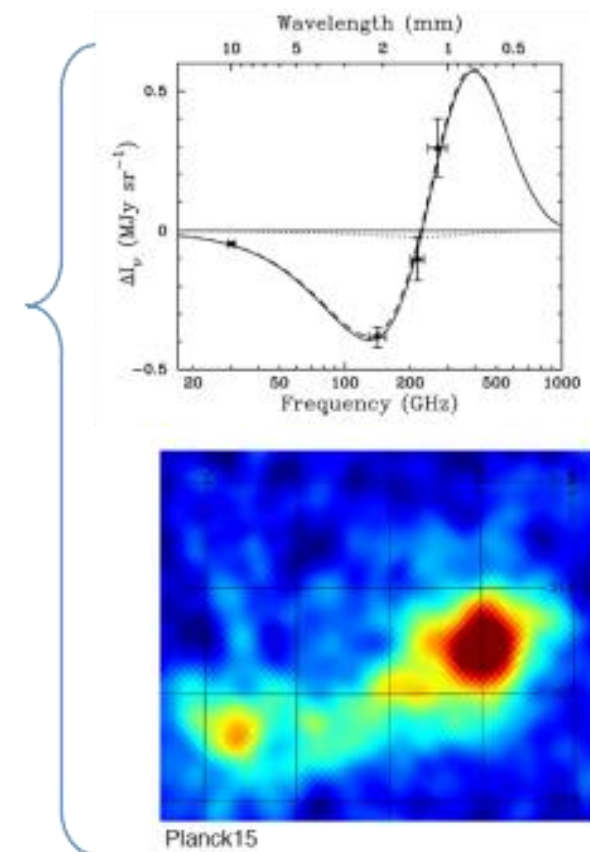
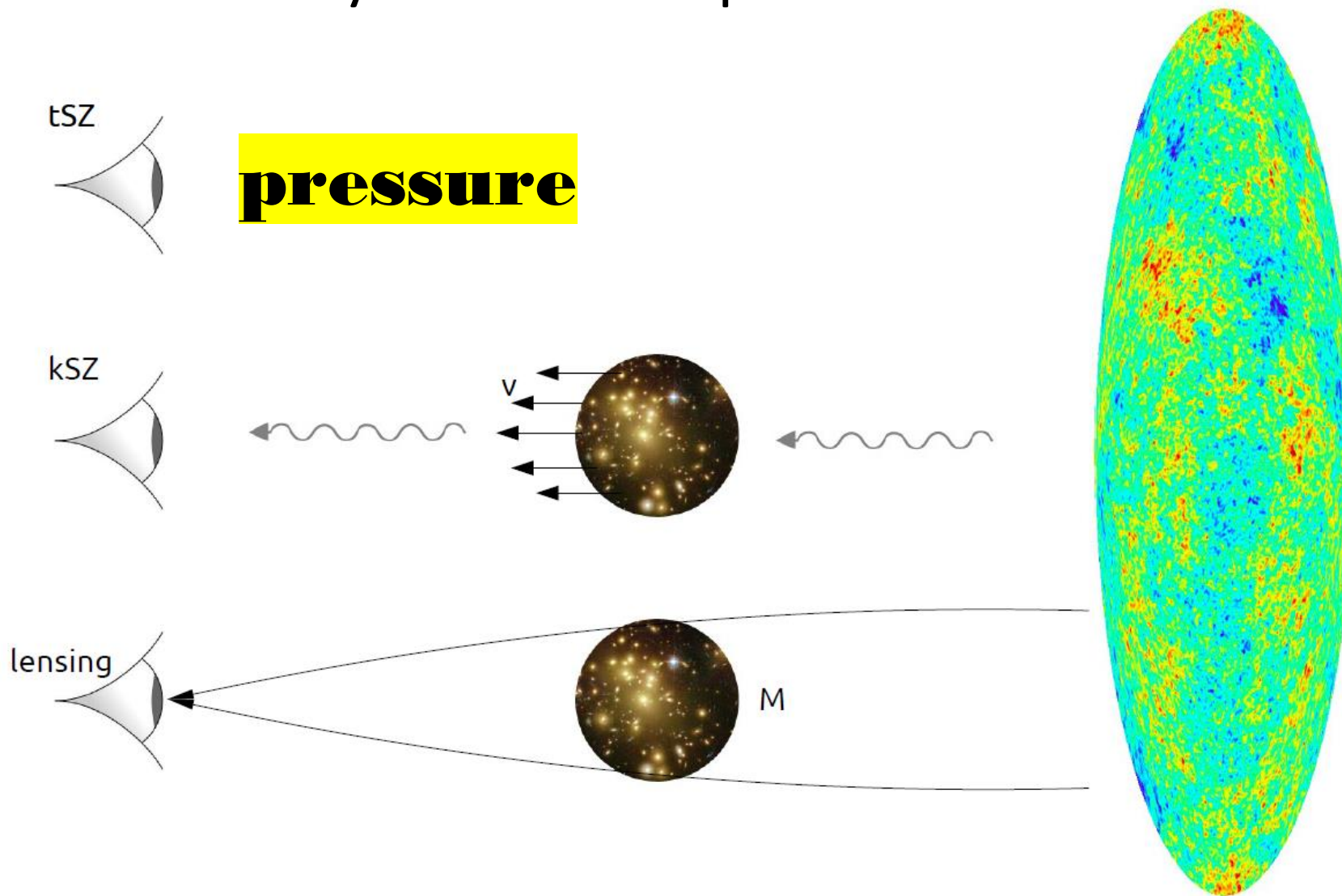


# Secondary anisotropies of the CMB



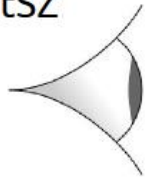
Planck15

# Secondary anisotropies of the CMB

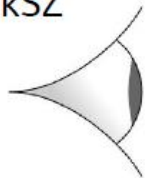


# Secondary anisotropies of the CMB

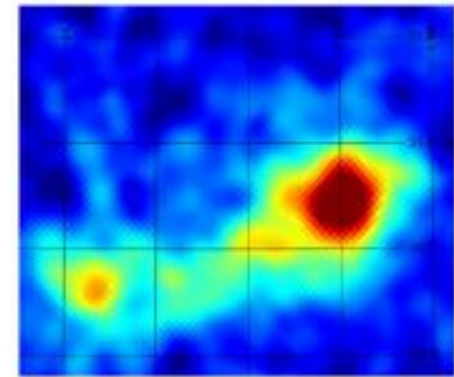
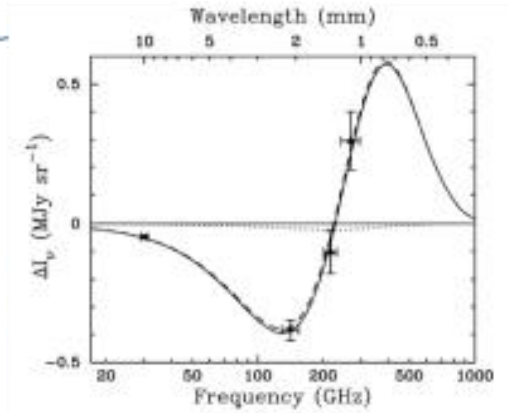
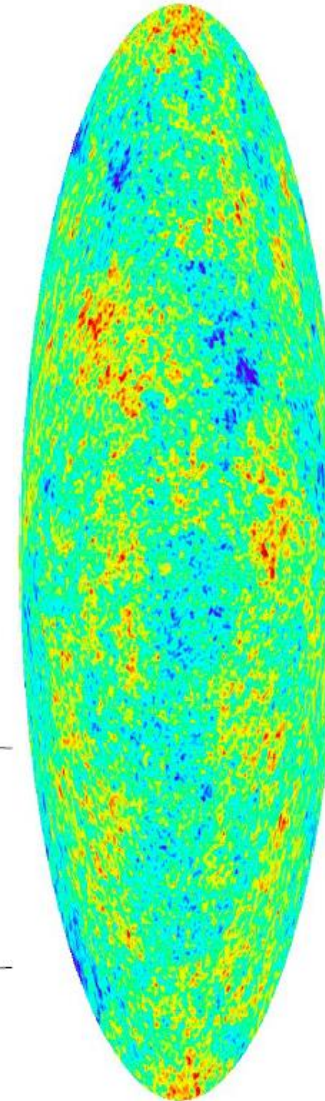
tSZ

**pressure**

kSZ

**gas density**

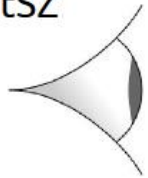
lensing



Planck15

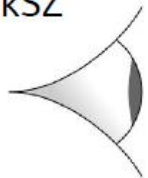
# Secondary anisotropies of the CMB

tSZ



**pressure**

kSZ

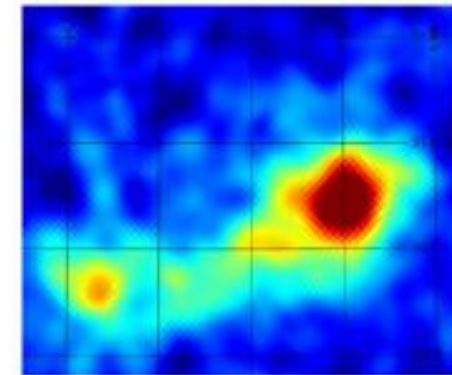
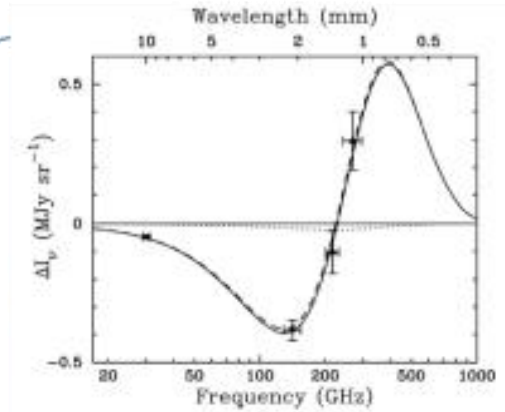
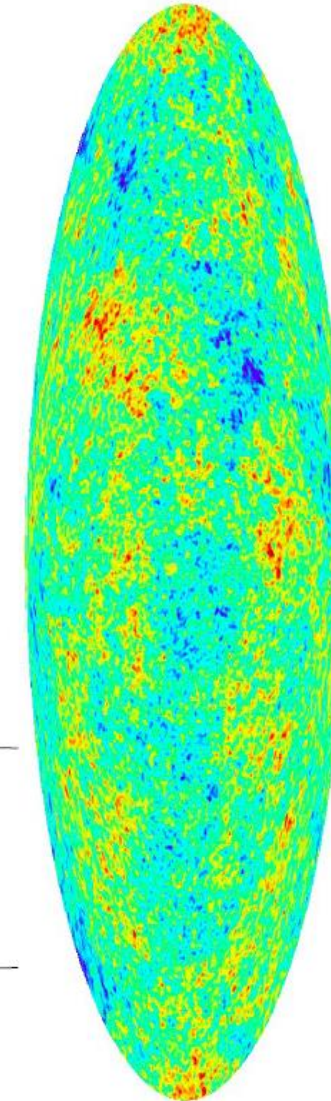


**gas density**

lensing



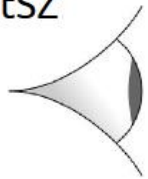
**matter density**



Planck15

# Secondary anisotropies of the CMB

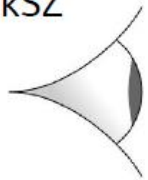
tSZ



$$\left. \frac{\Delta T}{T} \right|_{\text{tSZ}}(\nu, \hat{\mathbf{n}}) = f_{\text{tSZ}}(\nu) \frac{\sigma_T}{m_e c^2} \int P_e(l_z, \hat{\mathbf{n}}) dl_z$$

$$\equiv f_{\text{tSZ}}(\nu) y(\hat{\mathbf{n}})$$

kSZ



$$\left. \frac{\Delta T}{T} \right|_{\text{kSZ}}(\hat{\mathbf{n}}) = -\sigma_T \int (\boldsymbol{\beta} \cdot \hat{\mathbf{n}}) n_e(l_z, \hat{\mathbf{n}}) dl_z$$

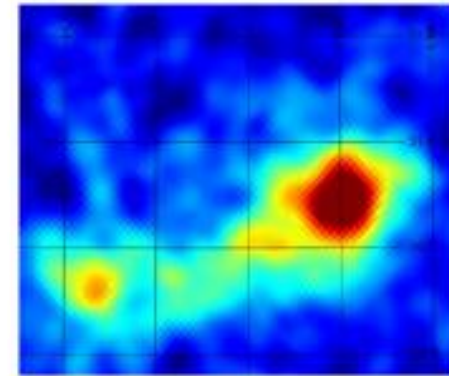
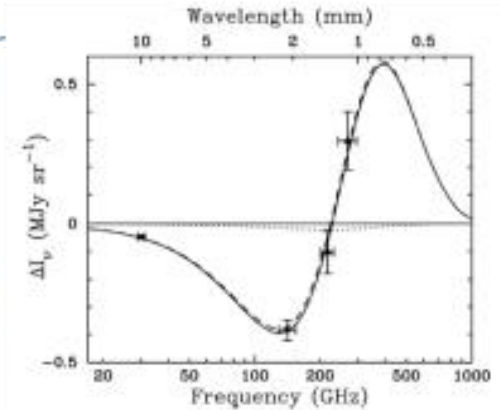
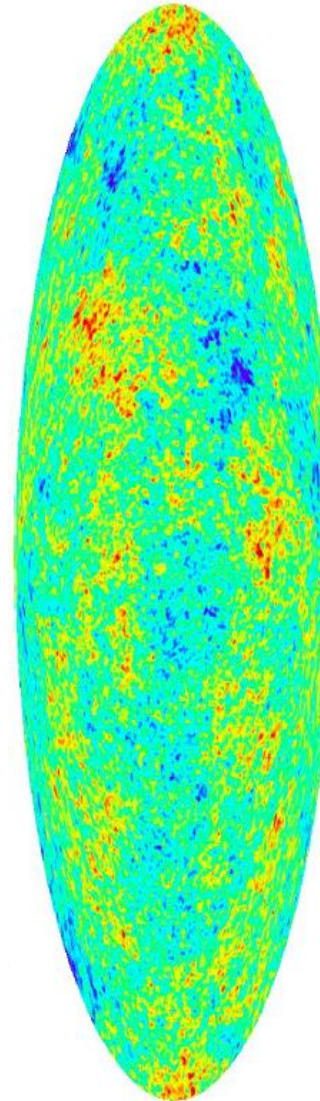
$$\equiv -\beta_r \tau(\hat{\mathbf{n}}),$$

lensing



$$\kappa(\mathbf{x}) = \Sigma(\mathbf{x}) / \Sigma_{\text{crit}}$$

$$\Sigma(\mathbf{x}) \equiv \int_{-\infty}^{\infty} dl \rho(l, \mathbf{x}), \quad \Sigma_{\text{crit}} \equiv \frac{c^2 d_S}{4\pi G d_L d_{LS}}$$



Planck15

# Secondary anisotropies of the CMB



$$\left. \frac{\Delta T}{T} \right|_{\text{tSZ}}(\nu, \hat{\mathbf{n}}) = f_{\text{tSZ}}(\nu) \frac{\sigma_T}{m_e c^2} \int P_e(l_z, \hat{\mathbf{n}}) dl_z$$

$$\equiv f_{\text{tSZ}}(\nu) y(\hat{\mathbf{n}})$$



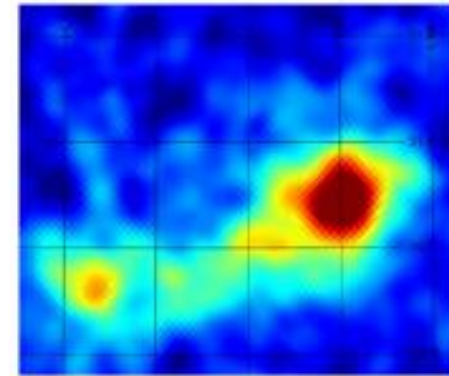
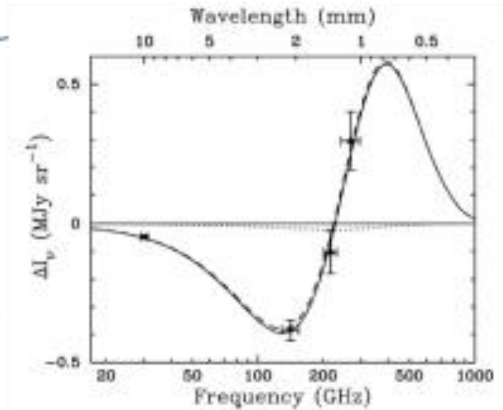
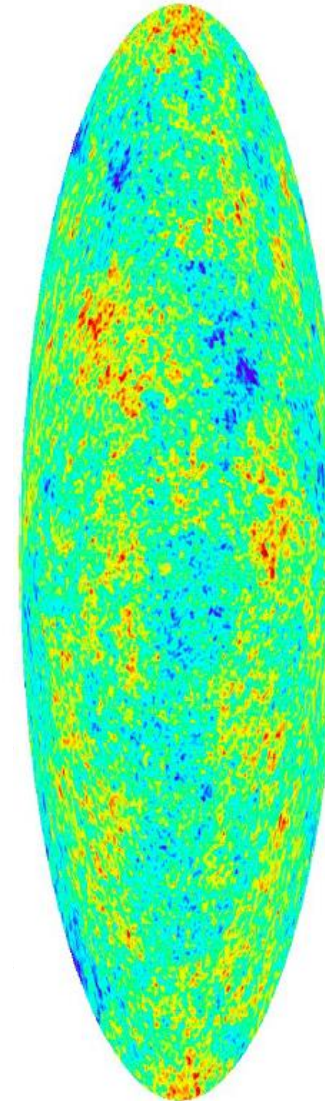
$$\left. \frac{\Delta T}{T} \right|_{\text{kSZ}}(\hat{\mathbf{n}}) = -\sigma_T \int (\boldsymbol{\beta} \cdot \hat{\mathbf{n}}) n_e(l_z, \hat{\mathbf{n}}) dl_z$$

$$\equiv -\beta_r \tau(\hat{\mathbf{n}}),$$



$$\kappa(\mathbf{x}) = \Sigma(\mathbf{x}) / \Sigma_{\text{crit}}$$

$$\Sigma(\mathbf{x}) \equiv \int_{-\infty}^{\infty} dl \rho(l, \mathbf{x}), \quad \Sigma_{\text{crit}} \equiv \frac{c^2 d_S}{4\pi G d_L d_{LS}}$$



Planck15

thermal Sunyaev Zel'dovich (tSZ)

$$y(\hat{\boldsymbol{\theta}}) = \frac{\sigma_T}{m_e c^2} \int \frac{d\chi}{1+z} P_e(\chi \hat{\boldsymbol{\theta}})$$

# thermal Sunyaev Zel'dovich (tSZ)

$$y(\hat{\theta}) = \frac{\sigma_T}{m_e c^2} \int \frac{d\chi}{1+z} P_e(\chi \hat{\theta})$$

Measure gas  
pressure

Link to mass

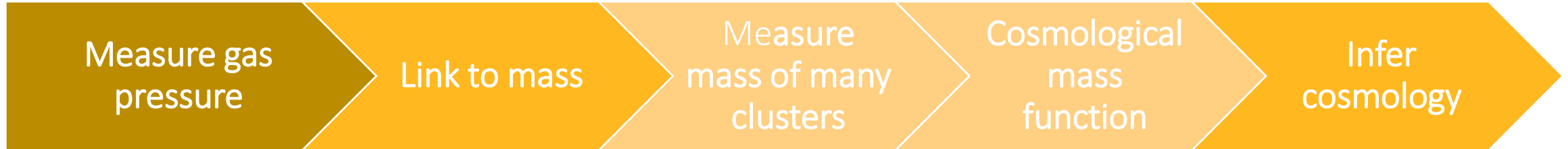
Measure  
mass of many  
clusters

Cosmological  
mass  
function

Infer  
cosmology

# thermal Sunyaev Zel'dovich (tSZ)

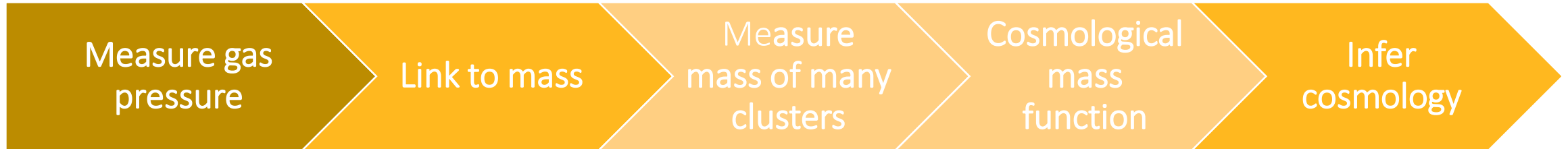
$$y(\hat{\theta}) = \frac{\sigma_T}{m_e c^2} \int \frac{d\chi}{1+z} P_e(\chi \hat{\theta})$$



- ✓ Easy to measure
- ✓ Good mass proxy

# thermal Sunyaev Zel'dovich (tSZ)

$$y(\hat{\theta}) = \frac{\sigma_T}{m_e c^2} \int \frac{d\chi}{1+z} P_e(\chi \hat{\theta})$$



- ✓ Easy to measure
- ✓ Good mass proxy

$$E^{-\beta}(z) \left[ \frac{D_A^2(z) \bar{Y}_{500}}{10^{-4} \text{ Mpc}^2} \right] = Y_* \left[ \frac{h}{0.7} \right]^{-2+\alpha} \left[ \frac{(1-b) M_{500}}{6 \times 10^{14} M_\odot} \right]^\alpha$$

*Planck Coll et al. 1502.01596*

- ✗ Calibrate  $y$ - $M$  relation
- ✗ *hydrostatic mass bias*

# What have we done?

$$y(\hat{\boldsymbol{\theta}}) = \frac{\sigma_T}{m_e c^2} \int \frac{d\chi}{1+z} P_e(\chi \hat{\boldsymbol{\theta}})$$

- ✓ Cross-correlations of **galaxy clustering** with **tSZ** from Planck

# What have we done?

- ✓ Cross-correlations of **galaxy clustering** with **tSZ** from Planck

$$y(\hat{\theta}) = \frac{\sigma_T}{m_e c^2} \int \frac{d\chi}{1+z} P_e(\chi \hat{\theta})$$

$$\delta_g(\hat{\theta}) = \int \delta z \varphi_g(z) \Delta_g(\chi(z), \hat{\theta})$$

# What have we done?

- ✓ Cross-correlations of **galaxy clustering** with **tSZ** from Planck

$$y(\hat{\theta}) = \frac{\sigma_T}{m_e c^2} \int \frac{d\chi}{1+z} P_e(\chi \hat{\theta})$$

$$\delta_g(\hat{\theta}) = \int \delta z \varphi_g(z) \Delta_g(\chi(z), \hat{\theta})$$

galaxy bias

$$C_l^{gg} \propto b_g^2$$

hydrostatic mass bias

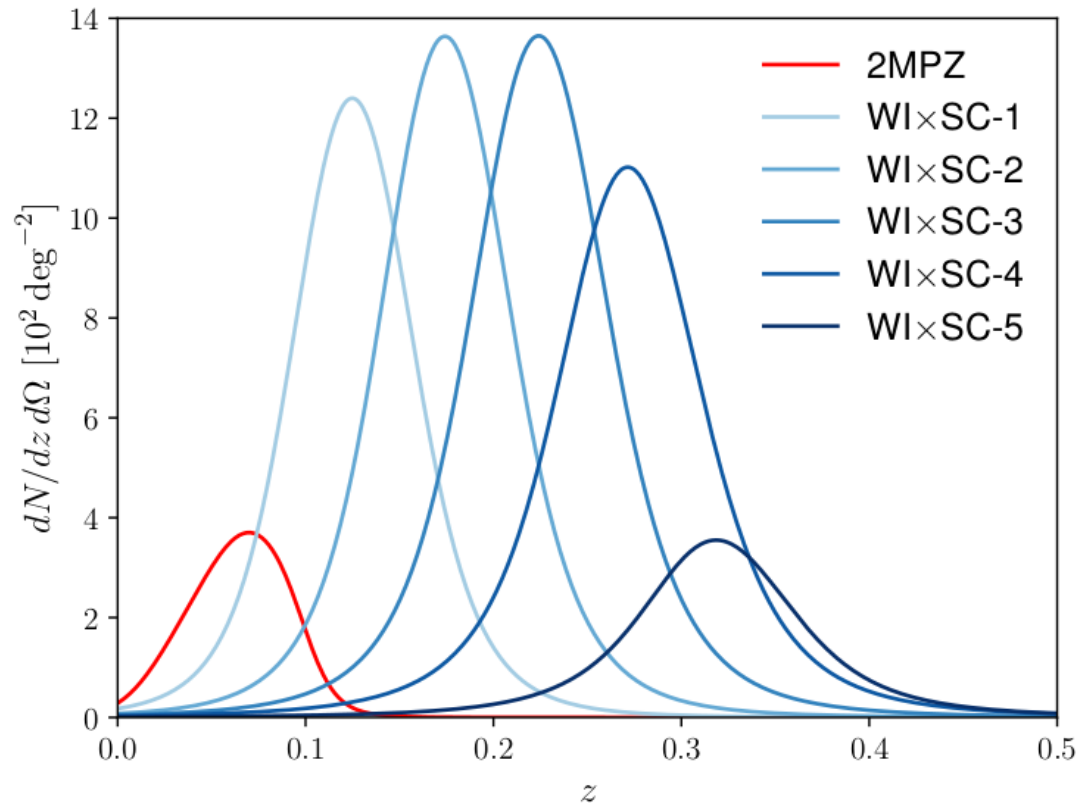
$$C_l^{gy} \propto b_g (1 - b_H)^\alpha$$

# What have we done?

- ✓ Cross-correlations of **galaxy clustering** with **tSZ** from Planck
- ✓ 20 million galaxies – split them in **redshift bins** to measure **evolution**

$$y(\hat{\theta}) = \frac{\sigma_T}{m_e c^2} \int \frac{d\chi}{1+z} P_e(\chi \hat{\theta})$$

$$\delta_g(\hat{\theta}) = \int \delta z \varphi_g(z) \Delta_g(\chi(z), \hat{\theta})$$



galaxy bias

$$C_l^{gg} \propto b_g^2$$

hydrostatic mass bias

$$C_l^{gy} \propto b_g (1 - b_H)^\alpha$$

# Galaxies

$$\delta_g(\hat{\theta}) = \int \delta z \varphi_g(z) \Delta_g(\chi(z), \hat{\theta})$$

# Galaxies

## Number Distribution

Halo Occupation Distribution

[Berlind & Weinberg 2002](#), [Zheng et al. 2005](#), [van den Bosch et al. 2013](#)

## Density Profile

NFW Profile

[Navarro, Frenk, White 1996](#)

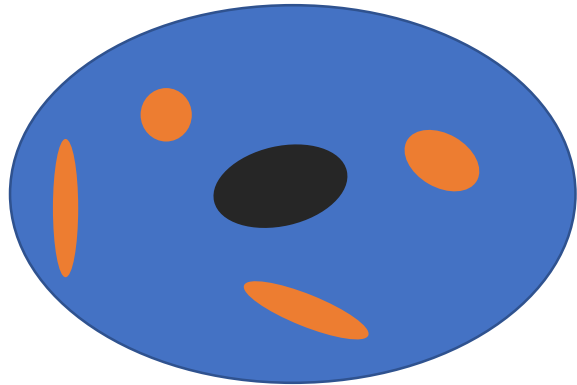
$$\delta_g(\hat{\theta}) = \int \delta z \varphi_g(z) \Delta_g(\chi(z), \hat{\theta})$$

# Galaxies

## Number Distribution

Halo Occupation Distribution

Berlind & Weinberg 2002, Zheng et al. 2005, van den Bosch et al. 2013



$$\langle N_c(M) \rangle = \frac{1}{2} \left[ 1 + \operatorname{erf} \left( \frac{\log(M/M_{\min})}{\sigma_{\ln M}} \right) \right]$$

$$\langle N_s(M) \rangle = \Theta(M - M_0) \left( \frac{M - M_0}{M'_1} \right)^{\alpha_s}$$

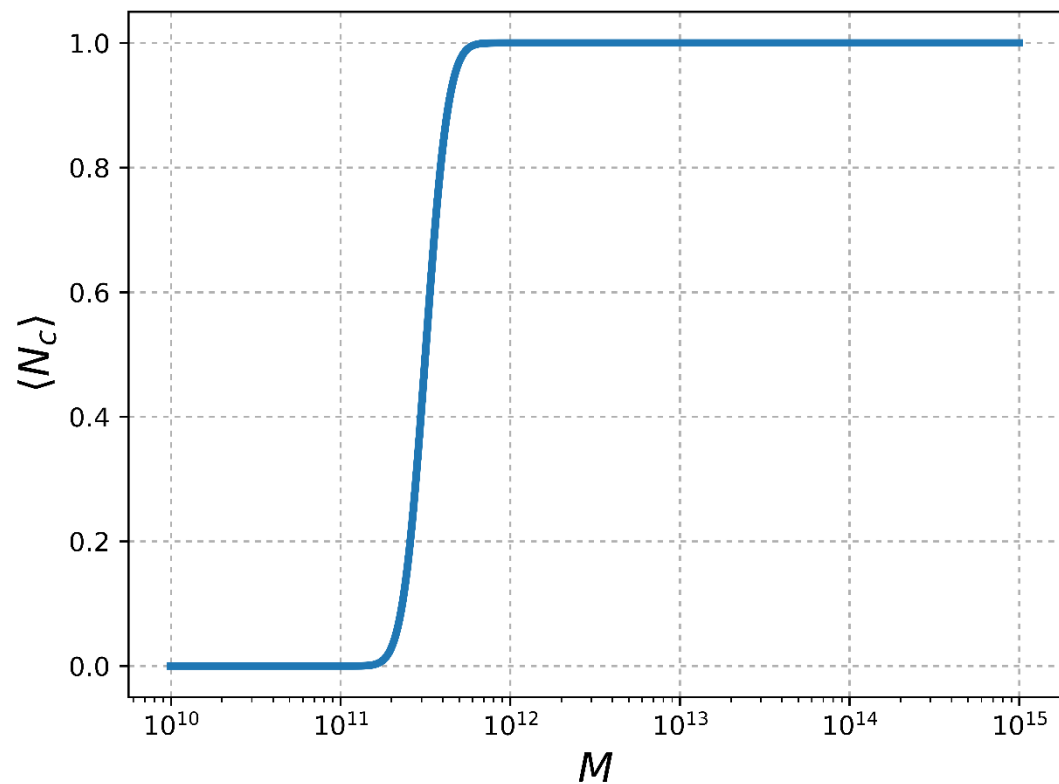
$$\delta_g(\hat{\theta}) = \int \delta z \varphi_g(z) \Delta_g(\chi(z), \hat{\theta})$$

## Density Profile

NFW Profile

Navarro, Frenk, White 1996

# Galaxies



$$\langle N_s(M) \rangle = \Theta(M - M_0) \left( \frac{M - M_0}{M'_1} \right)^{\alpha_s}$$

$$\delta_g(\hat{\theta}) = \int \delta z \varphi_g(z) \Delta_g(\chi(z), \hat{\theta})$$

## Density Profile

NFW Profile

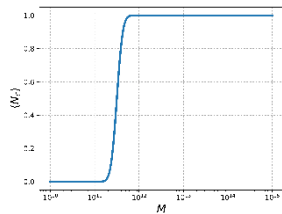
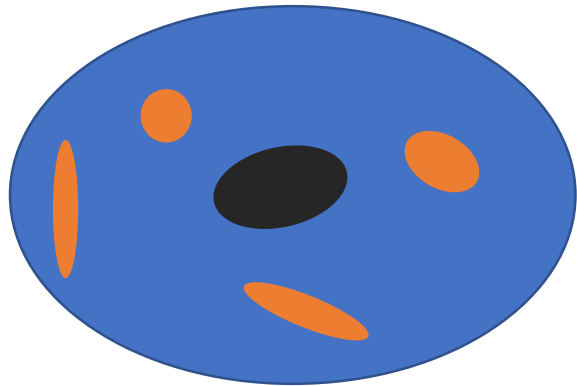
Navarro, Frenk, White 1996

# Galaxies

## Number Distribution

Halo Occupation Distribution

Berlind & Weinberg 2002, Zheng et al. 2005, van den Bosch et al. 2013



$$\langle N_c(M) \rangle = \frac{1}{2} \left[ 1 + \operatorname{erf} \left( \frac{\log(M/M_{\min})}{\sigma_{\ln M}} \right) \right]$$

$$\langle N_s(M) \rangle = \Theta(M - M_0) \left( \frac{M - M_0}{M'_1} \right)^{\alpha_s}$$

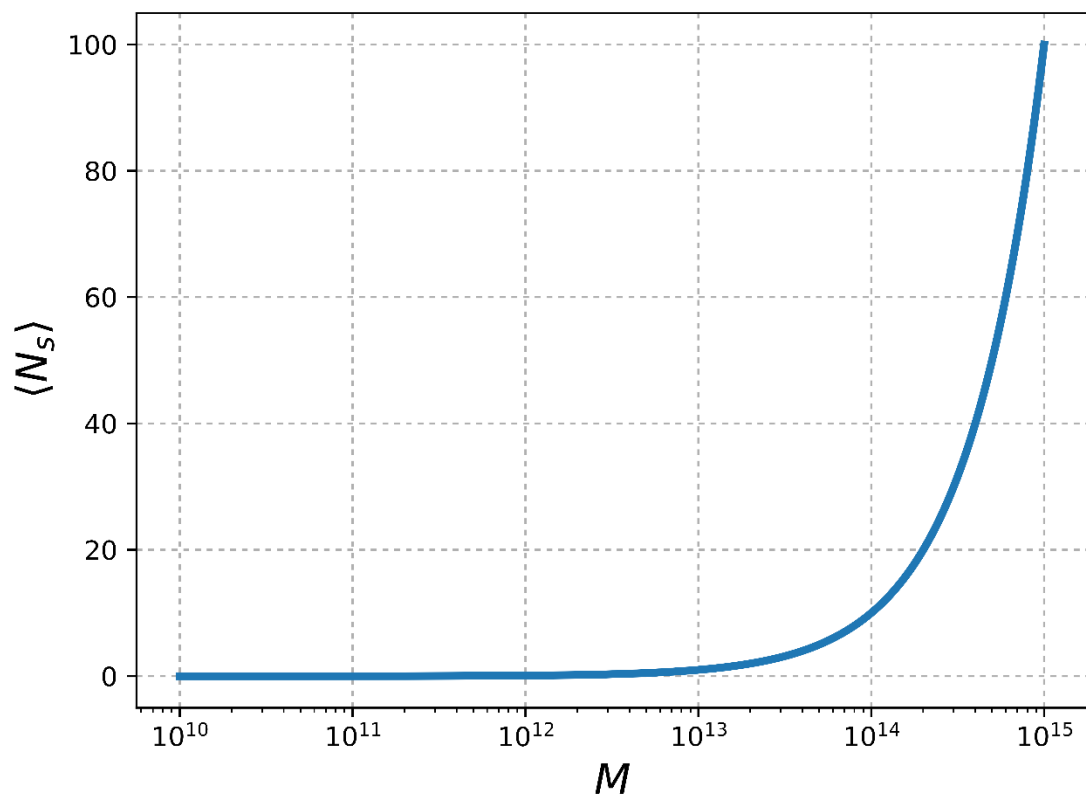
$$\delta_g(\hat{\theta}) = \int \delta z \varphi_g(z) \Delta_g(\chi(z), \hat{\theta})$$

## Density Profile

NFW Profile

Navarro, Frenk, White 1996

# Galaxies



$$\langle N_s(M) \rangle = \Theta(M - M_0) \left( \frac{M - M_0}{M'_1} \right)^{\alpha_s}$$

$$\delta_g(\hat{\theta}) = \int \delta z \varphi_g(z) \Delta_g(\chi(z), \hat{\theta})$$

## Density Profile

### NFW Profile

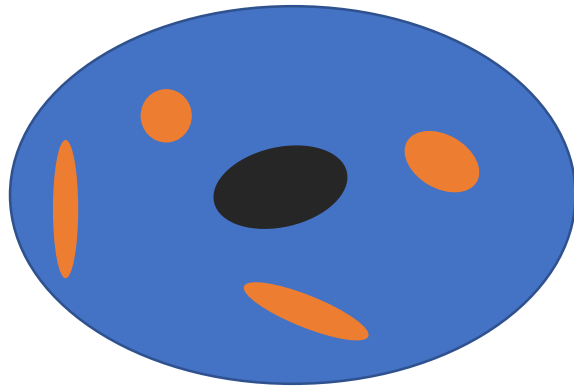
Navarro, Frenk, White 1996

# Galaxies

## Number Distribution

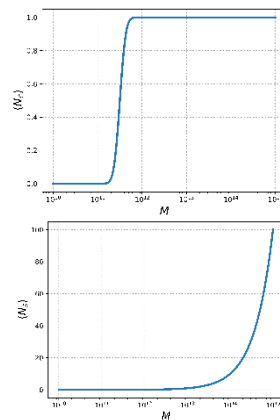
Halo Occupation Distribution

Berlind & Weinberg 2002, Zheng et al. 2005, van den Bosch et al. 2013



$$\langle N_c(M) \rangle = \frac{1}{2} \left[ 1 + \operatorname{erf} \left( \frac{\log(M/M_{\min})}{\sigma_{\ln M}} \right) \right]$$

$$\langle N_s(M) \rangle = \Theta(M - M_0) \left( \frac{M - M_0}{M'_1} \right)^{\alpha_s}$$



$$\delta_g(\hat{\theta}) = \int \delta z \varphi_g(z) \Delta_g(\chi(z), \hat{\theta})$$

## Density Profile

NFW Profile

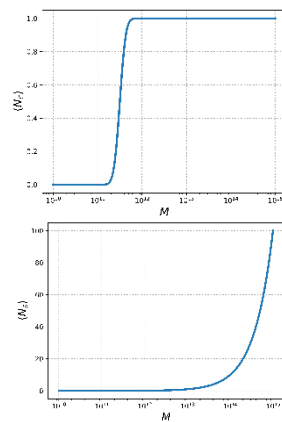
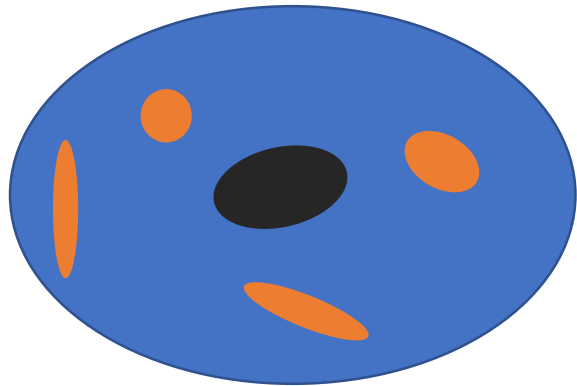
Navarro, Frenk, White 1996

# Galaxies

## Number Distribution

Halo Occupation Distribution

Berlind & Weinberg 2002, Zheng et al. 2005, van den Bosch et al. 2013



$$\langle N_c(M) \rangle = \frac{1}{2} \left[ 1 + \operatorname{erf} \left( \frac{\log(M/M_{\min})}{\sigma_{\ln M}} \right) \right]$$

$$\langle N_s(M) \rangle = \Theta(M - M_0) \left( \frac{M - M_0}{M'_1} \right)^{\alpha_s}$$

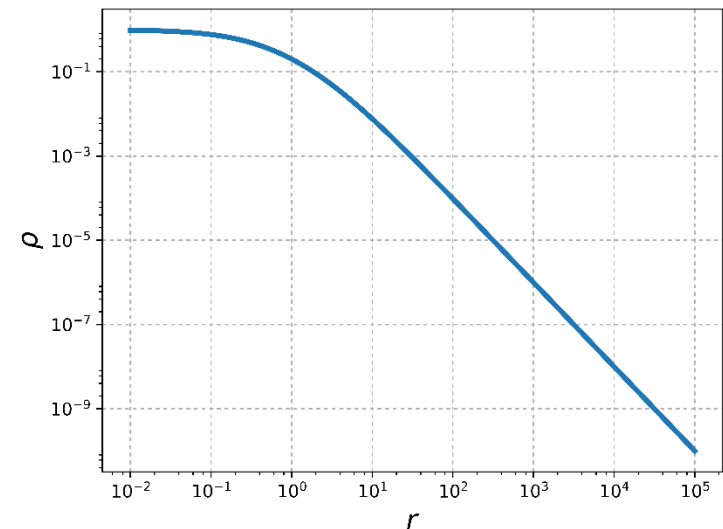
## Density Profile

NFW Profile

Navarro, Frenk, White 1996

$$\delta_g(\hat{\theta}) = \int \delta z \varphi_g(z) \Delta_g(\chi(z), \hat{\theta})$$

$$\rho_r = \frac{\rho_0}{\frac{r}{R_s} \left( 1 + \frac{r}{R_s} \right)^2}$$



## tSZ

$$y(\hat{\theta}) = \frac{\sigma_T}{m_e c^2} \int \frac{d\chi}{1+z} P_e(\chi \hat{\theta})$$

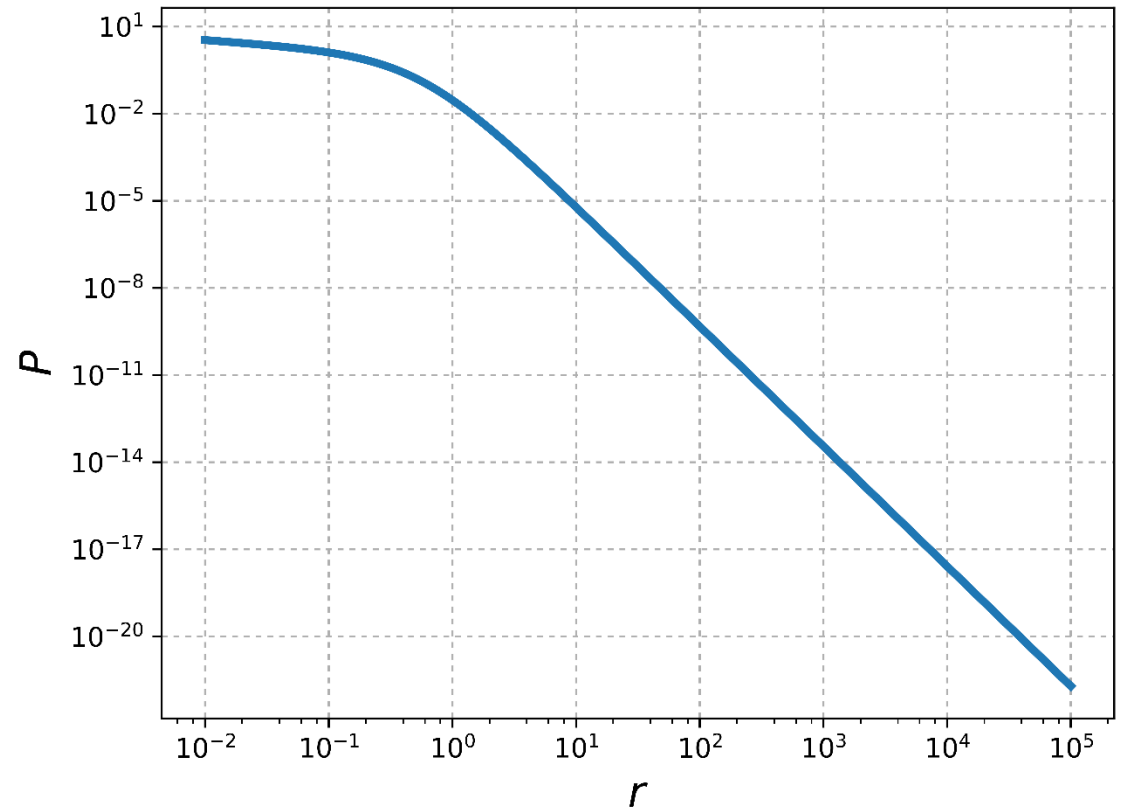
## Pressure Profile

generalised NFW Profile

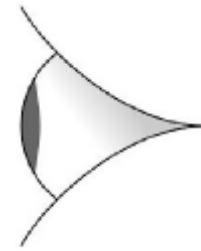
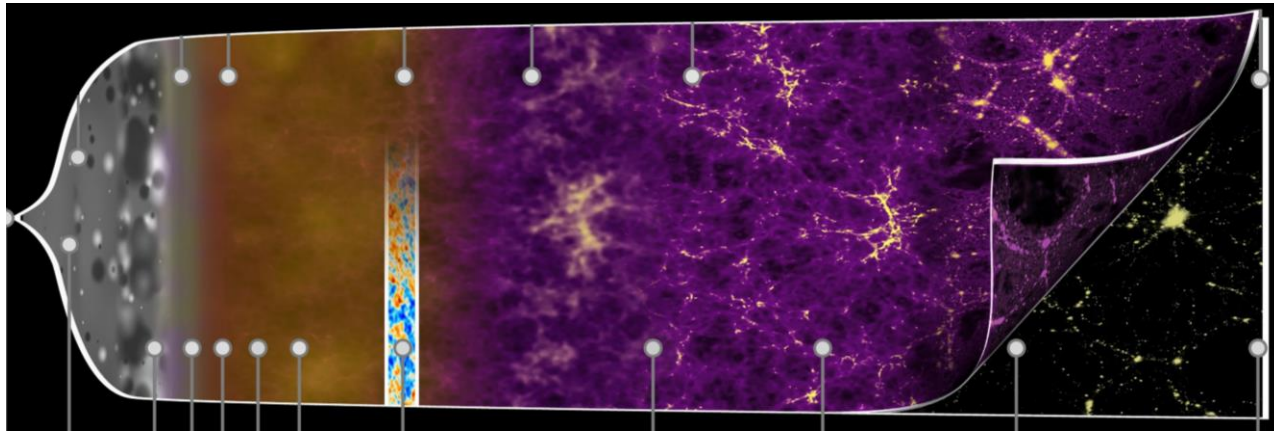
Arnaud et al. 2010, Planck Collaboration et al. 2016

$$P_e(r) = P_* p(r/r_{500c})$$

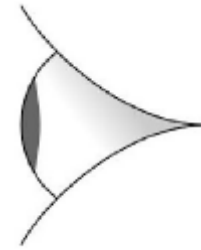
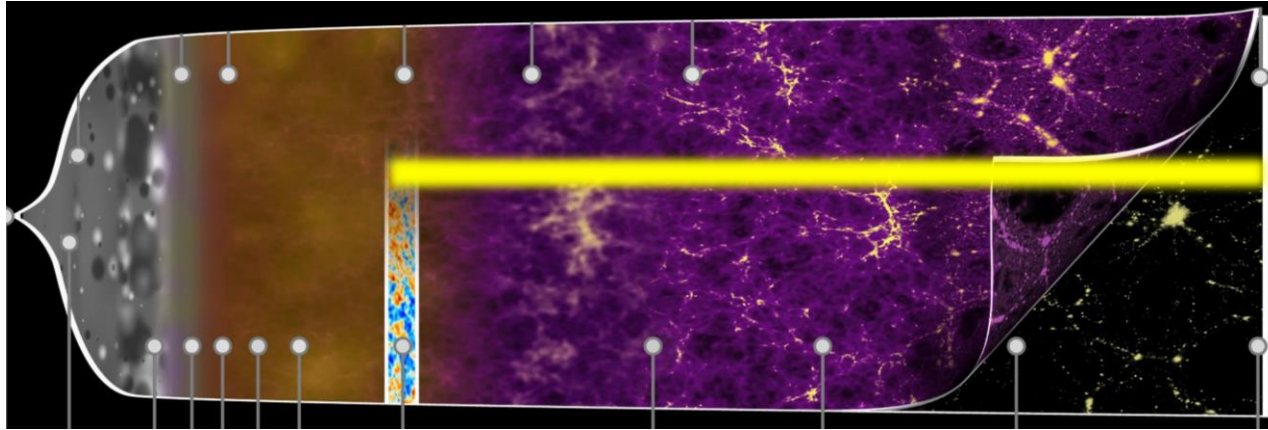
$$\left\{ \begin{array}{l} P_* = 6.41 (1.65 \text{ eV cm}^{-3}) h_{70}^{8/3} \left( \frac{h_{70} (1 - b_H) M_{500c}}{3 \times 10^{14} M_\odot} \right)^{0.79} \\ p(x) = (c_P x)^{-\gamma} (1 + (c_P x)^\alpha)^{(\gamma - \beta)/\alpha} \end{array} \right.$$



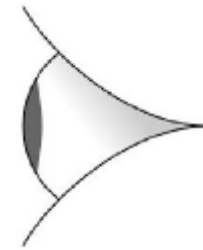
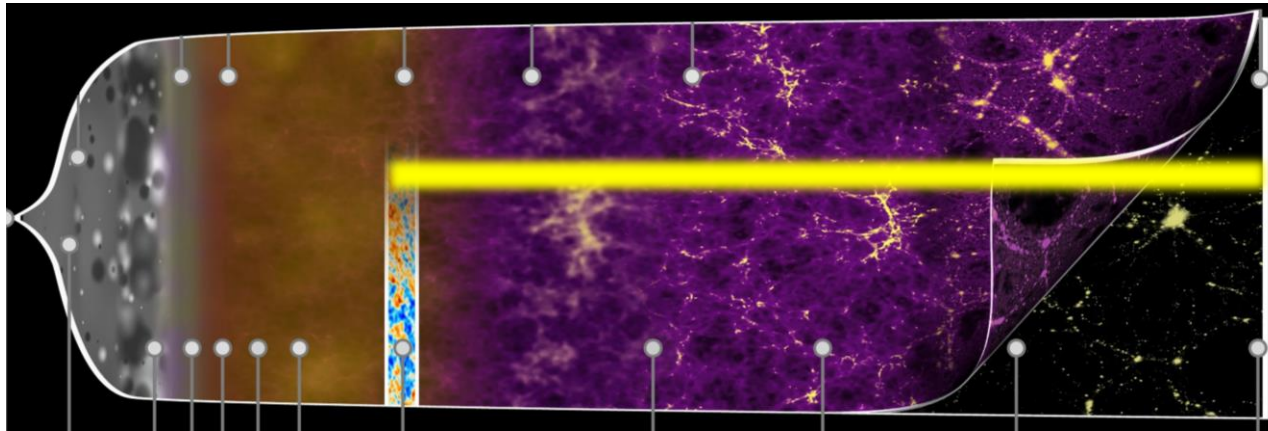
# 3D $\rightarrow$ 2D



# 3D $\rightarrow$ 2D

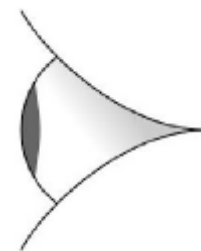
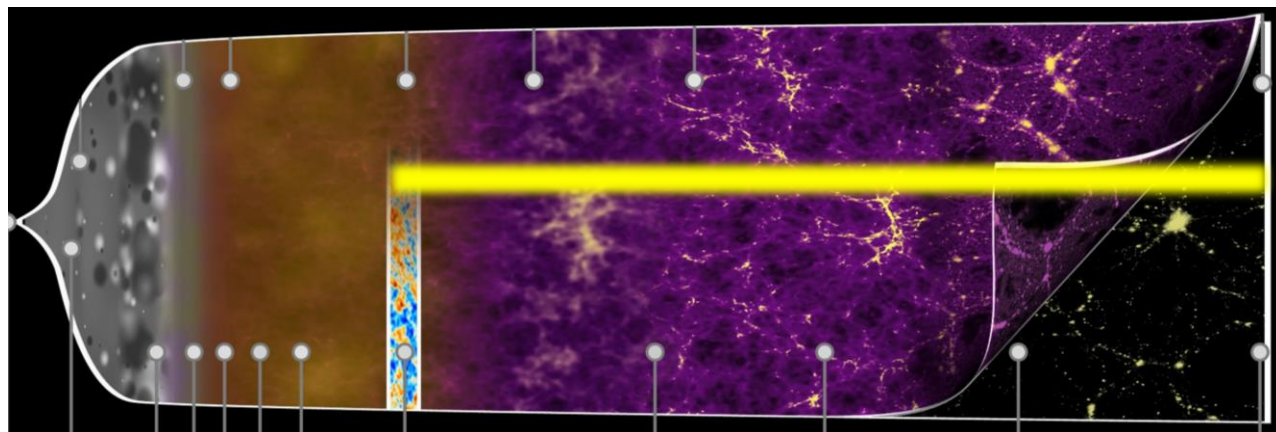


# 3D $\rightarrow$ 2D

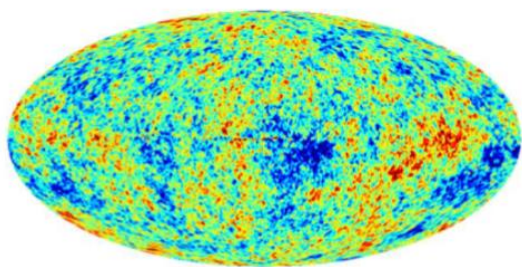


$$u(\hat{\theta}) = \int d\chi W_u U(\chi\hat{\theta})$$

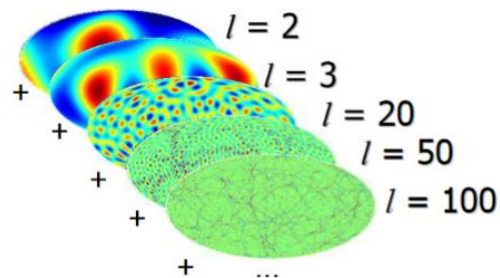
# 3D $\rightarrow$ 2D



$$u(\hat{\theta}) = \int d\chi W_u U(\chi\hat{\theta})$$



=



$$C_l^{uv} = \int d\chi \frac{W_u W_v}{\chi^2} P_{UV}(k, z)$$

# The Halo Model

$$C_l^{uv} = \int d\chi \frac{W_u W_v}{\chi^2} P_{UV}(k, z)$$

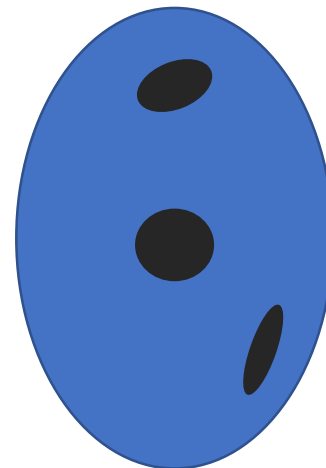
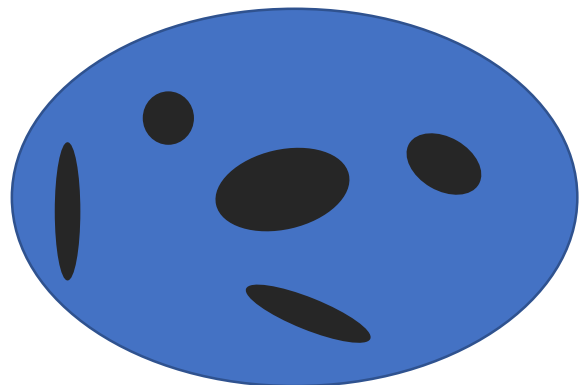
# The Halo Model

$$P_{UV}(k) = P_{UV}^{1h}(k) + P_{UV}^{2h}(k)$$

$$C_l^{uv} = \int d\chi \frac{W_u W_v}{\chi^2} P_{UV}(k, z)$$

# The Halo Model

$P^{2h}$

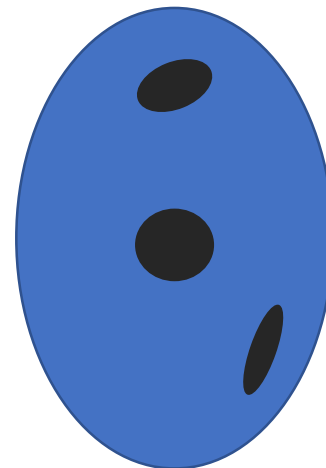
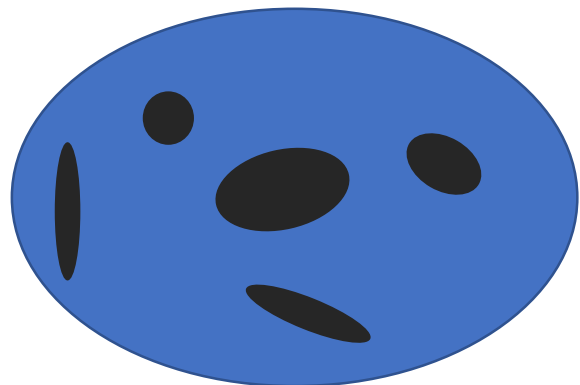


$$P_{UV}(k) = P_{UV}^{1h}(k) + P_{UV}^{2h}(k)$$

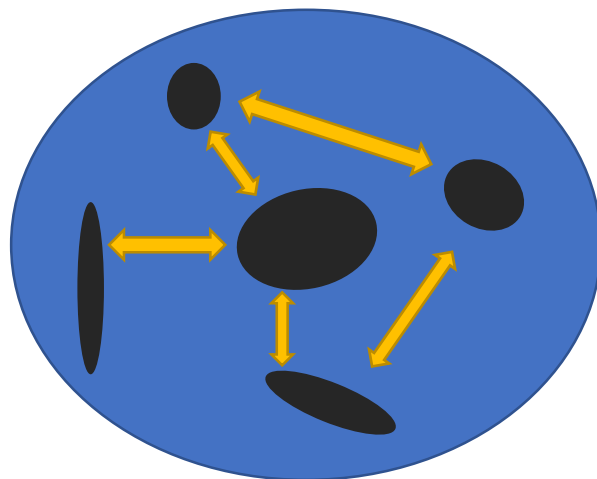
$$C_l^{uv} = \int d\chi \frac{W_u W_v}{\chi^2} P_{UV}(k, z)$$

# The Halo Model

$P^{2h}$



$P^{1h}$

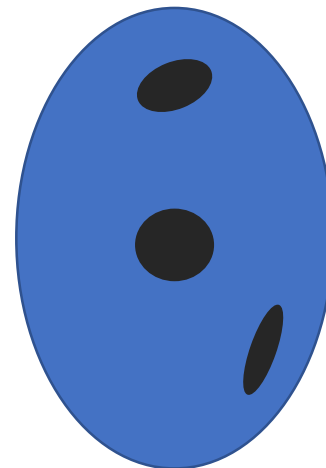
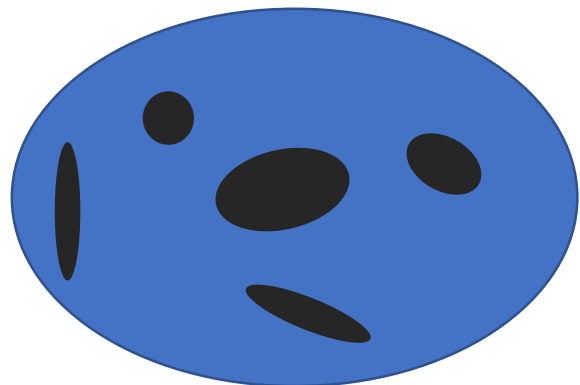


$$P_{UV}(k) = P_{UV}^{1h}(k) + P_{UV}^{2h}(k)$$

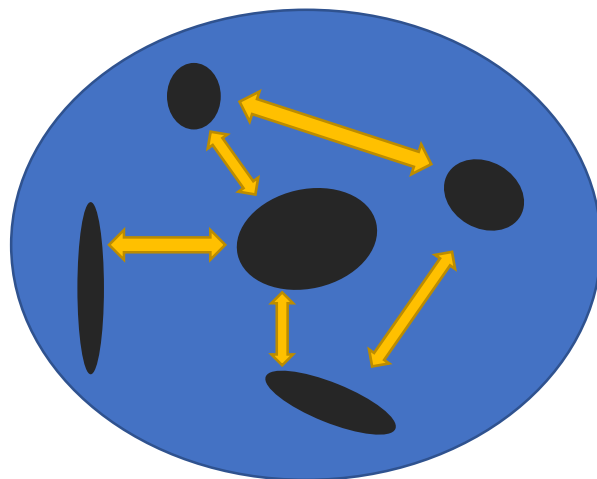
$$C_l^{uv} = \int d\chi \frac{W_u W_v}{\chi^2} P_{UV}(k, z)$$

# The Halo Model

**P<sup>2h</sup>**



**P<sup>1h</sup>**



$$P_{UV}^{1h}(k) = \int dM \frac{dn}{dM} \langle U(k|M) V(k|M) \rangle$$

$$P_{UV}^{2h}(k) = \langle b_U \rangle \langle b_V \rangle P_L(k)$$

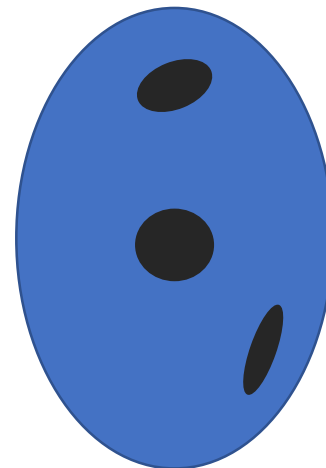
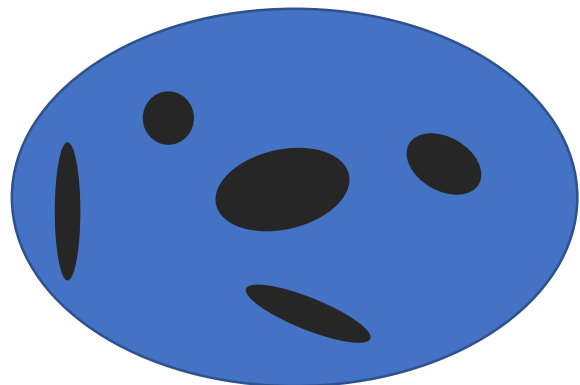
$$\langle b_U \rangle = \int dM \frac{dn}{dM} b_h(M) \langle U(k|M) \rangle$$

$$P_{UV}(k) = P_{UV}^{1h}(k) + P_{UV}^{2h}(k)$$

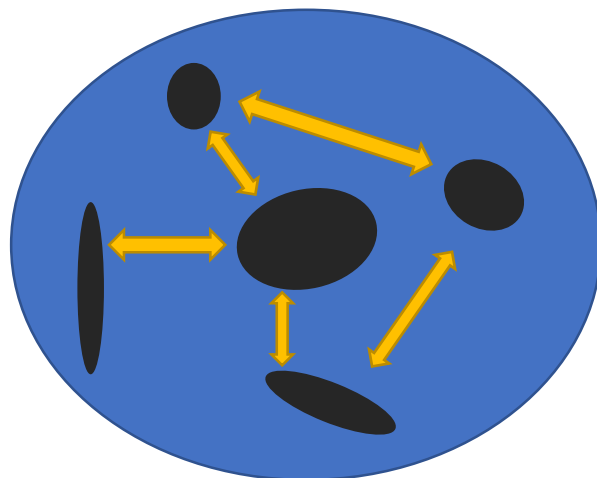
$$C_l^{uv} = \int d\chi \frac{W_u W_v}{\chi^2} P_{UV}(k, z)$$

# The Halo Model

$P^{2h}$



$P^{1h}$



$$P_{UV}^{1h}(k) = \int dM \frac{dn}{dM} \langle U(k|M) V(k|M) \rangle$$

$$P_{UV}^{2h}(k) = \langle b_U \rangle \langle b_V \rangle P_L(k)$$

$$\langle b_U \rangle = \int dM \frac{dn}{dM} b_h(M) \langle U(k|M) \rangle$$

$$P_{UV}(k) = P_{UV}^{1h}(k) + P_{UV}^{2h}(k)$$

$$C_l^{uv} = \int d\chi \frac{W_u W_v}{\chi^2} P_{UV}(k, z)$$

$$\langle b_{Pe} \rangle = \int dM \frac{dn}{dM} b_h(M) E_T(M)$$





# Corrections

Halo transition regime	Calibrate from Simulations <a href="#">Takahashi et al. 2012</a>

$$R(k) \equiv \frac{P_{\text{Halofit}}(k)}{P_{\text{halo model}}(k)}$$

# Corrections

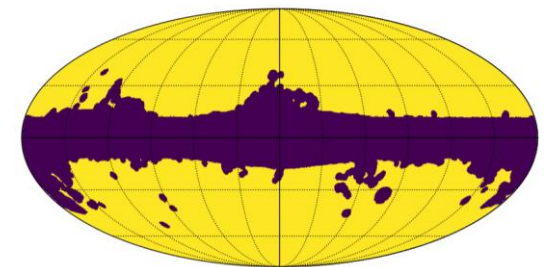
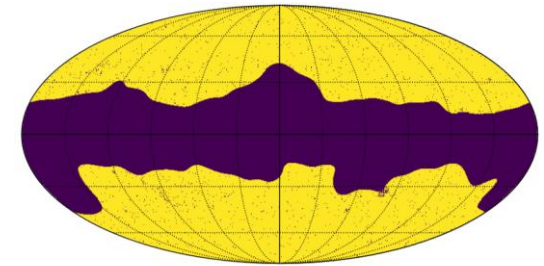
<b>Halo transition regime</b>	Calibrate from Simulations <a href="#">Takahashi et al. 2012</a>
<b>Star contamination</b>	

$$R(k) \equiv \frac{P_{\text{Halofit}}(k)}{P_{\text{halo model}}(k)}$$

# Corrections

<b>Halo transition regime</b>	Calibrate from Simulations <a href="#">Takahashi et al. 2012</a>
<b>Star contamination</b>	Mask, Smooth scale dependence <a href="#">Peacock &amp; Bilicki 2018</a>

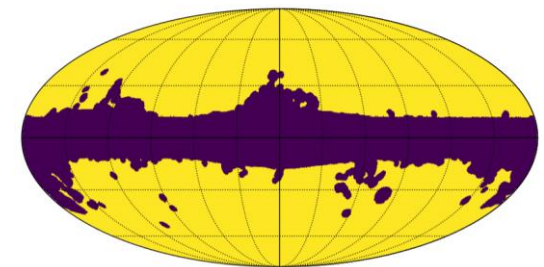
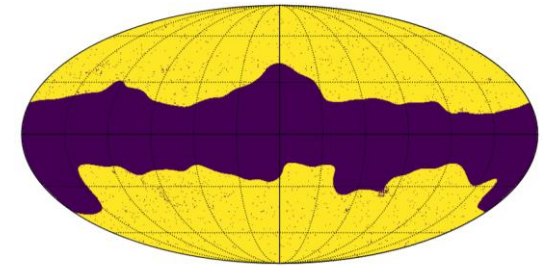
$$R(k) \equiv \frac{P_{\text{Halofit}}(k)}{P_{\text{halo model}}(k)}$$



# Corrections

<b>Halo transition regime</b>	Calibrate from Simulations <a href="#">Takahashi et al. 2012</a>
<b>Star contamination</b>	Mask, Smooth scale dependence <a href="#">Peacock &amp; Bilicki 2018</a>
<b>Residual star contamination</b>	

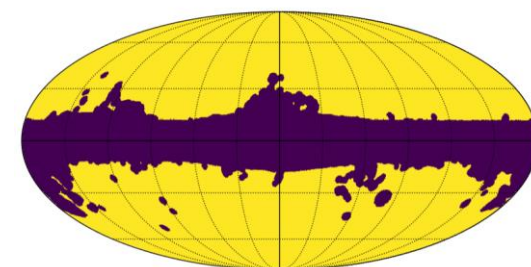
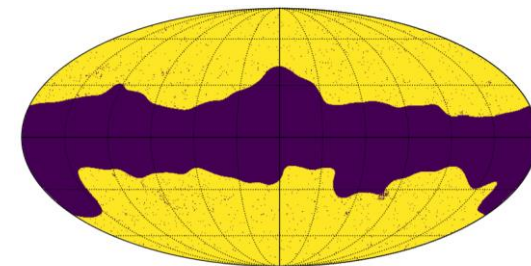
$$R(k) \equiv \frac{P_{\text{Halofit}}(k)}{P_{\text{halo model}}(k)}$$



# Corrections

<b>Halo transition regime</b>	Calibrate from Simulations <a href="#">Takahashi et al. 2012</a>
<b>Star contamination</b>	Mask, Smooth scale dependence <a href="#">Peacock &amp; Bilicki 2018</a>
<b>Residual star contamination</b>	Deproject star map <a href="#">Elsner et al. 2017</a> <a href="#">Alonso et al. 2019</a>

$$R(k) \equiv \frac{P_{\text{Halofit}}(k)}{P_{\text{halo model}}(k)}$$

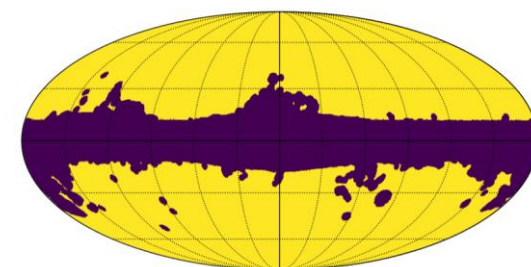
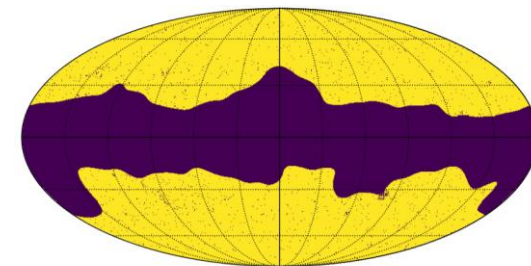


$$\mathbf{m}_{\text{obs}} = \mathbf{m}_{\text{true}} + \epsilon \mathbf{t}$$

# Corrections

Halo transition regime	Calibrate from Simulations <a href="#">Takahashi et al. 2012</a>
Star contamination	Mask, Smooth scale dependence <a href="#">Peacock &amp; Bilicki 2018</a>
Residual star contamination	Deproject star map <a href="#">Elsner et al. 2017</a> <a href="#">Alonso et al. 2019</a>
Reddening	

$$R(k) \equiv \frac{P_{\text{Halofit}}(k)}{P_{\text{halo model}}(k)}$$

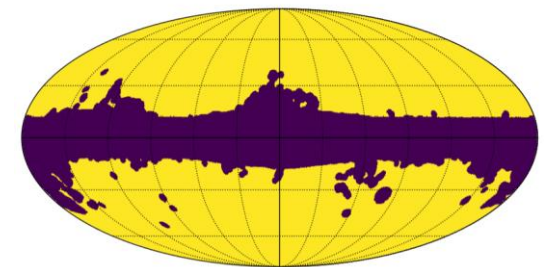
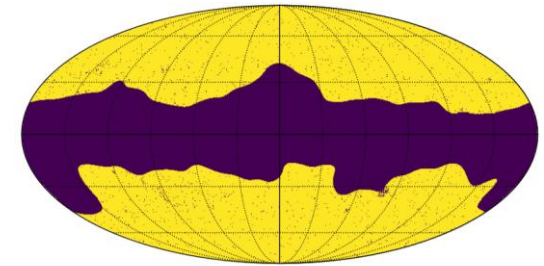


$$\mathbf{m}_{\text{obs}} = \mathbf{m}_{\text{true}} + \epsilon \mathbf{t}$$

# Corrections

<b>Halo transition regime</b>	Calibrate from Simulations <a href="#">Takahashi et al. 2012</a>
<b>Star contamination</b>	Mask, Smooth scale dependence <a href="#">Peacock &amp; Bilicki 2018</a>
<b>Residual star contamination</b>	Deproject star map <a href="#">Elsner et al. 2017</a> <a href="#">Alonso et al. 2019</a>
<b>Reddening</b>	Deproject dust map <a href="#">Elsner et al. 2017</a> <a href="#">Alonso et al. 2019</a>

$$R(k) \equiv \frac{P_{\text{Halofit}}(k)}{P_{\text{halo model}}(k)}$$

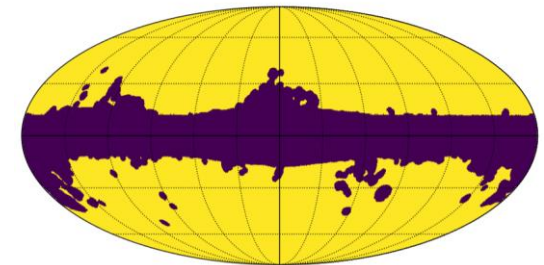
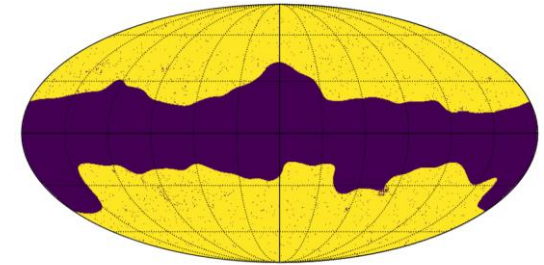


$$\mathbf{m}_{\text{obs}} = \mathbf{m}_{\text{true}} + \epsilon \mathbf{t}$$

# Corrections

<b>Halo transition regime</b>	Calibrate from Simulations <a href="#">Takahashi et al. 2012</a>
<b>Star contamination</b>	Mask, Smooth scale dependence <a href="#">Peacock &amp; Bilicki 2018</a>
<b>Residual star contamination</b>	Deproject star map <a href="#">Elsner et al. 2017</a> <a href="#">Alonso et al. 2019</a>
<b>Reddening</b>	Deproject dust map <a href="#">Elsner et al. 2017</a> <a href="#">Alonso et al. 2019</a>
<b>Modulation on photographic plates</b>	

$$R(k) \equiv \frac{P_{\text{Halofit}}(k)}{P_{\text{halo model}}(k)}$$

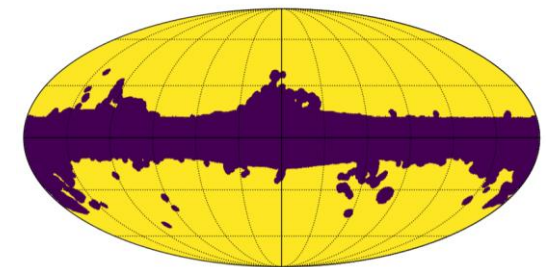
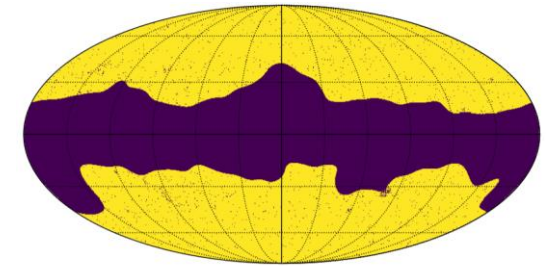


$$\mathbf{m}_{\text{obs}} = \mathbf{m}_{\text{true}} + \epsilon \mathbf{t}$$

# Corrections

<b>Halo transition regime</b>	Calibrate from Simulations <a href="#">Takahashi et al. 2012</a>
<b>Star contamination</b>	Mask, Smooth scale dependence <a href="#">Peacock &amp; Bilicki 2018</a>
<b>Residual star contamination</b>	Deproject star map <a href="#">Elsner et al. 2017</a> <a href="#">Alonso et al. 2019</a>
<b>Reddening</b>	Deproject dust map <a href="#">Elsner et al. 2017</a> <a href="#">Alonso et al. 2019</a>
<b>Modulation on photographic plates</b>	Model on power spectrum

$$R(k) \equiv \frac{P_{\text{Halofit}}(k)}{P_{\text{halo model}}(k)}$$



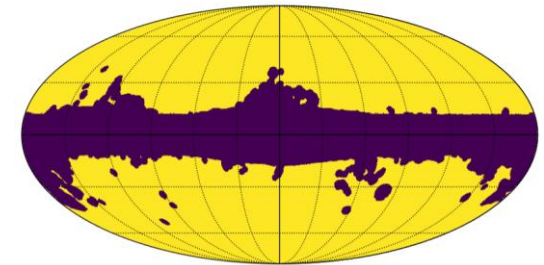
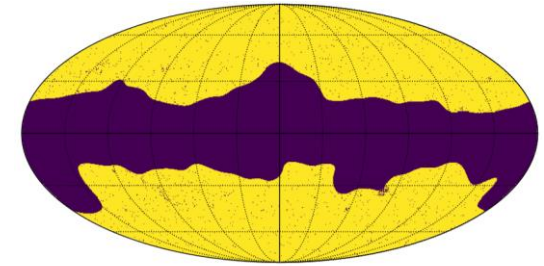
$$C_{\ell}^{\text{plate}} = \sigma_{\text{plate}}^2 S_{\text{plate}} \exp \left[ (-\ell \theta_{\text{plate}})^2 / 12 \right]$$

$$\mathbf{m}_{\text{obs}} = \mathbf{m}_{\text{true}} + \epsilon \mathbf{t}$$

# Corrections

Halo transition regime	Calibrate from Simulations <a href="#">Takahashi et al. 2012</a>
Star contamination	Mask, Smooth scale dependence <a href="#">Peacock &amp; Bilicki 2018</a>
Residual star contamination	Deproject star map <a href="#">Elsner et al. 2017</a> <a href="#">Alonso et al. 2019</a>
Reddening	Deproject dust map <a href="#">Elsner et al. 2017</a> <a href="#">Alonso et al. 2019</a>
Modulation on photographic plates	Model on power spectrum
Theoretical limitations	

$$R(k) \equiv \frac{P_{\text{Halofit}}(k)}{P_{\text{halo model}}(k)}$$



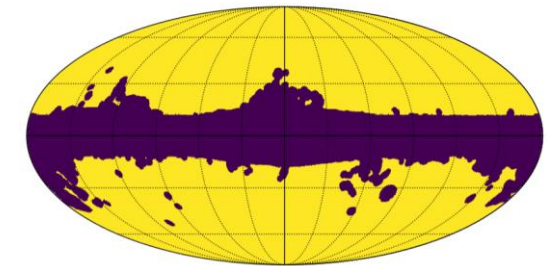
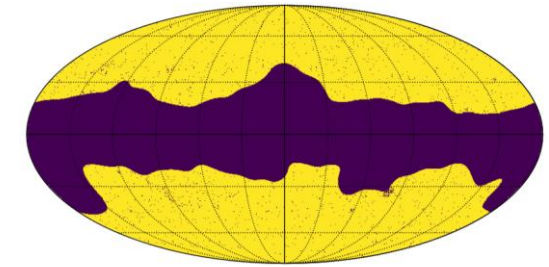
$$C_{\ell}^{\text{plate}} = \sigma_{\text{plate}}^2 S_{\text{plate}} \exp \left[ (-\ell \theta_{\text{plate}})^2 / 12 \right]$$

$$\mathbf{m}_{\text{obs}} = \mathbf{m}_{\text{true}} + \epsilon \mathbf{t}$$

# Corrections

<b>Halo transition regime</b>	Calibrate from Simulations <a href="#">Takahashi et al. 2012</a>
<b>Star contamination</b>	Mask, Smooth scale dependence <a href="#">Peacock &amp; Bilicki 2018</a>
<b>Residual star contamination</b>	Deproject star map <a href="#">Elsner et al. 2017</a> <a href="#">Alonso et al. 2019</a>
<b>Reddening</b>	Deproject dust map <a href="#">Elsner et al. 2017</a> <a href="#">Alonso et al. 2019</a>
<b>Modulation on photographic plates</b>	Model on power spectrum
<b>Theoretical limitations</b>	Scale cuts <a href="#">Xavier et al. 2018</a>

$$R(k) \equiv \frac{P_{\text{Halofit}}(k)}{P_{\text{halo model}}(k)}$$



$$\ell_{\min} = 10$$

$$\ell_{\max} = \bar{\chi} k_{\max} - 1/2$$

$$k_{\max} = 1 \text{ Mpc}^{-1}$$

$$C_{\ell}^{\text{plate}} = \sigma_{\text{plate}}^2 S_{\text{plate}} \exp \left[ (-\ell \theta_{\text{plate}})^2 / 12 \right]$$

$$\mathbf{m}_{\text{obs}} = \mathbf{m}_{\text{true}} + \epsilon \mathbf{t}$$

motivation

analysis

results

conclusions

theory

models

likelihood

# Fit parameters

---

# Fit parameters

## HOD parameters

$$\langle N_c(M) \rangle = \frac{1}{2} \left[ 1 + \operatorname{erf} \left( \frac{\log(M/M_{\min})}{\sigma_{\ln M}} \right) \right]$$

$$\langle N_s(M) \rangle = \Theta(M - M_0) \left( \frac{M - M_0}{M'_1} \right)^{\alpha_s}$$

---

# Fit parameters

## HOD parameters

$$\langle N_c(M) \rangle = \frac{1}{2} \left[ 1 + \operatorname{erf} \left( \frac{\log(M/M_{\min})}{\sigma_{\ln M}} \right) \right]$$

$$\langle N_s(M) \rangle = \Theta(M - M_0) \left( \frac{M - M_0}{M_1'} \right)^{\alpha_s}$$

$$M_{\min} = M_0$$

$$10 \leq \log \frac{M_{\min}}{M_{\odot}} \leq 16$$

$$10 \leq \log \frac{M_1'}{M_{\odot}} \leq 16$$

# Fit parameters

## HOD parameters

$$\langle N_c(M) \rangle = \frac{1}{2} \left[ 1 + \operatorname{erf} \left( \frac{\log(M/M_{\min})}{\sigma_{\ln M}} \right) \right]$$

$$\langle N_s(M) \rangle = \Theta(M - M_0) \left( \frac{M - M_0}{M_1'} \right)^{\alpha_s}$$

$$M_{\min} = M_0$$

## Mass bias

$$P_e(r) = P_* p(r/r_{500c})$$

$$P_* = 6.41 (1.65 \text{ eV cm}^{-3}) h_{70}^{8/3} \left( \frac{h_{70} (1 - b_H) M_{500c}}{3 \times 10^{14} M_{\odot}} \right)^{0.79}$$

$$10 \leq \log \frac{M_{\min}}{M_{\odot}} \leq 16$$

$$10 \leq \log \frac{M_1'}{M_{\odot}} \leq 16$$

# Fit parameters

## HOD parameters

$$\langle N_c(M) \rangle = \frac{1}{2} \left[ 1 + \operatorname{erf} \left( \frac{\log(M/M_{\min})}{\sigma_{\ln M}} \right) \right]$$

$$\langle N_s(M) \rangle = \Theta(M - M_0) \left( \frac{M - M_0}{M_1'} \right)^{\alpha_s}$$

$$M_{\min} = M_0$$

## Mass bias

$$P_e(r) = P_* p(r/r_{500c})$$

$$P_* = 6.41 (1.65 \text{ eV cm}^{-3}) h_{70}^{8/3} \left( \frac{h_{70} (1 - b_H) M_{500c}}{3 \times 10^{14} M_{\odot}} \right)^{0.79}$$

$$10 \leq \log \frac{M_{\min}}{M_{\odot}} \leq 16$$

$$0 \leq (1 - b_H) \leq 0.99$$

$$10 \leq \log \frac{M_1'}{M_{\odot}} \leq 16$$

# Fit parameters

## HOD parameters

$$\langle N_c(M) \rangle = \frac{1}{2} \left[ 1 + \operatorname{erf} \left( \frac{\log(M/M_{\min})}{\sigma_{\ln M}} \right) \right]$$

$$\langle N_s(M) \rangle = \Theta(M - M_0) \left( \frac{M - M_0}{M_1} \right)^{\alpha_s}$$

$$M_{\min} = M_0$$

## Mass bias

$$P_e(r) = P_* p(r/r_{500c})$$

$$P_* = 6.41 (1.65 \text{ eV cm}^{-3}) h_{70}^{8/3} \left( \frac{h_{70}(1 - b_H) M_{500c}}{3 \times 10^{14} M_{\odot}} \right)^{0.79}$$

## 1h-covariance

$$P_{UV}^{1h}(k) = \int dM \frac{dn}{dM} \langle U(k|M) V(k|M) \rangle$$

$$10 \leq \log \frac{M_{\min}}{M_{\odot}} \leq 16$$

$$0 \leq (1 - b_H) \leq 0.99$$

$$10 \leq \log \frac{M_1'}{M_{\odot}} \leq 16$$

# Fit parameters

## HOD parameters

$$\langle N_c(M) \rangle = \frac{1}{2} \left[ 1 + \operatorname{erf} \left( \frac{\log(M/M_{\min})}{\sigma_{\ln M}} \right) \right]$$

$$\langle N_s(M) \rangle = \Theta(M - M_0) \left( \frac{M - M_0}{M_1'} \right)^{\alpha_s}$$

$$M_{\min} = M_0$$

## Mass bias

$$P_e(r) = P_* p(r/r_{500c})$$

$$P_* = 6.41 (1.65 \text{ eV cm}^{-3}) h_{70}^{8/3} \left( \frac{h_{70} (1 - b_H) M_{500c}}{3 \times 10^{14} M_{\odot}} \right)^{0.79}$$

## 1h-covariance

$$P_{UV}^{1h}(k) = \int dM \frac{dn}{dM} \langle U(k|M) V(k|M) \rangle$$

$$\langle u_y(k|M) u_g(k|M) \rangle = (1 + \rho_{yg}) \langle u_g(k|M) \rangle \langle u_y(k|M) \rangle$$

$$10 \leq \log \frac{M_{\min}}{M_{\odot}} \leq 16$$

$$0 \leq (1 - b_H) \leq 0.99$$

$$10 \leq \log \frac{M_1'}{M_{\odot}} \leq 16$$

# Fit parameters

## HOD parameters

$$\langle N_c(M) \rangle = \frac{1}{2} \left[ 1 + \operatorname{erf} \left( \frac{\log(M/M_{\min})}{\sigma_{\ln M}} \right) \right]$$

$$\langle N_s(M) \rangle = \Theta(M - M_0) \left( \frac{M - M_0}{M_1} \right)^{\alpha_s}$$

$$M_{\min} = M_0$$

## Mass bias

$$P_e(r) = P_* p(r/r_{500c})$$

$$P_* = 6.41 (1.65 \text{ eV cm}^{-3}) h_{70}^{8/3} \left( \frac{h_{70} (1 - b_H) M_{500c}}{3 \times 10^{14} M_{\odot}} \right)^{0.79}$$

## 1h-covariance

$$P_{UV}^{1h}(k) = \int dM \frac{dn}{dM} \langle U(k|M) V(k|M) \rangle$$

$$\langle u_y(k|M) u_g(k|M) \rangle = (1 + \rho_{yg}) \langle u_g(k|M) \rangle \langle u_y(k|M) \rangle$$

$$10 \leq \log \frac{M_{\min}}{M_{\odot}} \leq 16$$

$$0 \leq (1 - b_H) \leq 0.99$$

$$-1 \leq \rho_{yg} \leq 1$$

$$10 \leq \log \frac{M_1'}{M_{\odot}} \leq 16$$

# Fit parameters

## HOD parameters

$$\langle N_c(M) \rangle = \frac{1}{2} \left[ 1 + \operatorname{erf} \left( \frac{\log(M/M_{\min})}{\sigma_{\ln M}} \right) \right]$$

$$\langle N_s(M) \rangle = \Theta(M - M_0) \left( \frac{M - M_0}{M_1'} \right)^{\alpha_s}$$

$$M_{\min} = M_0$$

## Mass bias

$$P_e(r) = P_* p(r/r_{500c})$$

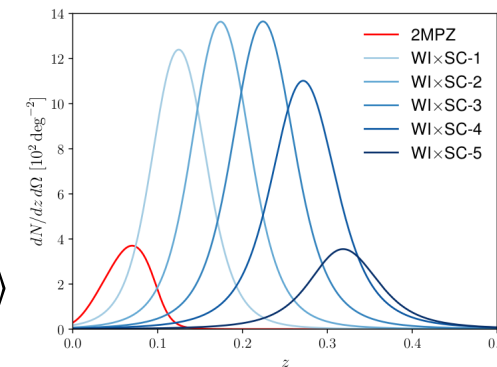
$$P_* = 6.41 (1.65 \text{ eV cm}^{-3}) h_{70}^{8/3} \left( \frac{h_{70} (1 - b_H) M_{500c}}{3 \times 10^{14} M_{\odot}} \right)^{0.79}$$

## 1h-covariance

$$P_{UV}^{1h}(k) = \int dM \frac{dn}{dM} \langle U(k|M) V(k|M) \rangle$$

$$\langle u_y(k|M) u_g(k|M) \rangle = (1 + \rho_{yg}) \langle u_g(k|M) \rangle \langle u_y(k|M) \rangle$$

## Redshift distribution uncertainties



$$10 \leq \log \frac{M_{\min}}{M_{\odot}} \leq 16$$

$$0 \leq (1 - b_H) \leq 0.99$$

$$-1 \leq \rho_{yg} \leq 1$$

$$10 \leq \log \frac{M_1'}{M_{\odot}} \leq 16$$

# Fit parameters

## HOD parameters

$$\langle N_c(M) \rangle = \frac{1}{2} \left[ 1 + \operatorname{erf} \left( \frac{\log(M/M_{\min})}{\sigma_{\ln M}} \right) \right]$$

$$\langle N_s(M) \rangle = \Theta(M - M_0) \left( \frac{M - M_0}{M_1'} \right)^{\alpha_s}$$

$$M_{\min} = M_0$$

## Mass bias

$$P_e(r) = P_* p(r/r_{500c})$$

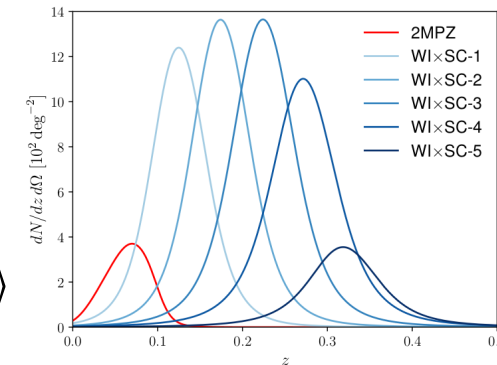
$$P_* = 6.41 (1.65 \text{ eV cm}^{-3}) h_{70}^{8/3} \left( \frac{h_{70} (1 - b_H) M_{500c}}{3 \times 10^{14} M_{\odot}} \right)^{0.79}$$

## 1h-covariance

$$P_{UV}^{1h}(k) = \int dM \frac{dn}{dM} \langle U(k|M) V(k|M) \rangle$$

$$\langle u_y(k|M) u_g(k|M) \rangle = (1 + \rho_{yg}) \langle u_g(k|M) \rangle \langle u_y(k|M) \rangle$$

## Redshift distribution uncertainties



$$p(z) \propto p_{\text{fid}} \left( \bar{z} + \frac{z - \bar{z}}{w_z} \right)$$

$$10 \leq \log \frac{M_{\min}}{M_{\odot}} \leq 16$$

$$0 \leq (1 - b_H) \leq 0.99$$

$$-1 \leq \rho_{yg} \leq 1$$

$$10 \leq \log \frac{M_1'}{M_{\odot}} \leq 16$$

# Fit parameters

## HOD parameters

$$\langle N_c(M) \rangle = \frac{1}{2} \left[ 1 + \operatorname{erf} \left( \frac{\log(M/M_{\min})}{\sigma_{\ln M}} \right) \right]$$

$$\langle N_s(M) \rangle = \Theta(M - M_0) \left( \frac{M - M_0}{M_1} \right)^{\alpha_s}$$

$$M_{\min} = M_0$$

## Mass bias

$$P_e(r) = P_* p(r/r_{500c})$$

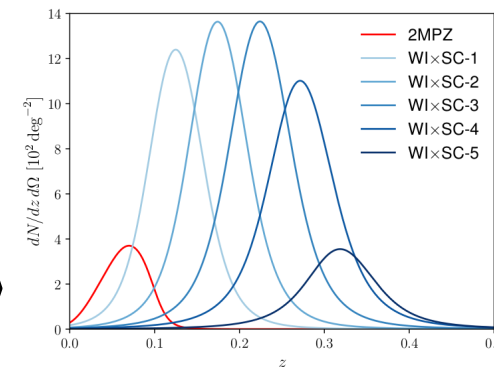
$$P_* = 6.41 (1.65 \text{ eV cm}^{-3}) h_{70}^{8/3} \left( \frac{h_{70}(1 - b_H) M_{500c}}{3 \times 10^{14} M_{\odot}} \right)^{0.79}$$

## 1h-covariance

$$P_{UV}^{1h}(k) = \int dM \frac{dn}{dM} \langle U(k|M) V(k|M) \rangle$$

$$\langle u_y(k|M) u_g(k|M) \rangle = (1 + \rho_{yg}) \langle u_g(k|M) \rangle \langle u_y(k|M) \rangle$$

## Redshift distribution uncertainties



$$p(z) \propto p_{\text{fid}} \left( \bar{z} + \frac{z - \bar{z}}{w_z} \right)$$

$$10 \leq \log \frac{M_{\min}}{M_{\odot}} \leq 16$$

$$0 \leq (1 - b_H) \leq 0.99$$

$$-1 \leq \rho_{yg} \leq 1$$

$$0.8 \leq w_z \leq 1.2$$

$$10 \leq \log \frac{M_1'}{M_{\odot}} \leq 16$$

# Likelihood function

$$-2 \log p(\mathbf{d}|\vec{\theta}) = \chi^2 \equiv (\mathbf{d} - \mathbf{t}(\vec{\theta}))^T \text{Cov}^{-1} (\mathbf{d} - \mathbf{t}(\vec{\theta}))$$

# Likelihood function

$$-2 \log p(\mathbf{d}|\vec{\theta}) = \chi^2 \equiv (\mathbf{d} - \mathbf{t}(\vec{\theta}))^T \text{Cov}^{-1} (\mathbf{d} - \mathbf{t}(\vec{\theta}))$$



**Gaussian**

$$\text{Cov}^G = \delta_{\ell\ell'} \frac{C_\ell^{uw} C_\ell^{vz} + C_\ell^{uz} C_\ell^{vw}}{2\ell + 1}$$

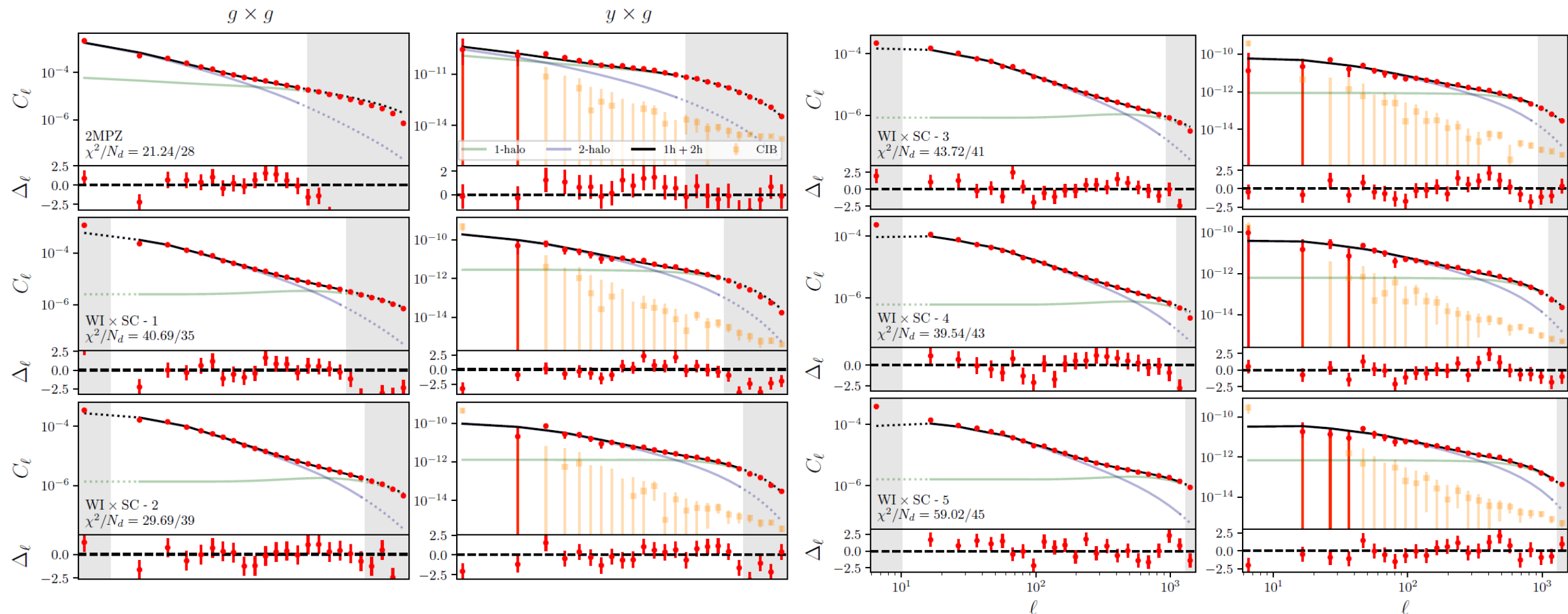
**non-Gaussian**

$$\text{Cov}^{\text{NG}} = \int d\chi \frac{W_u W_v W_w W_z}{4\pi f_{\text{sky}} \chi^6} \times T_{uvwz}^{1h}$$

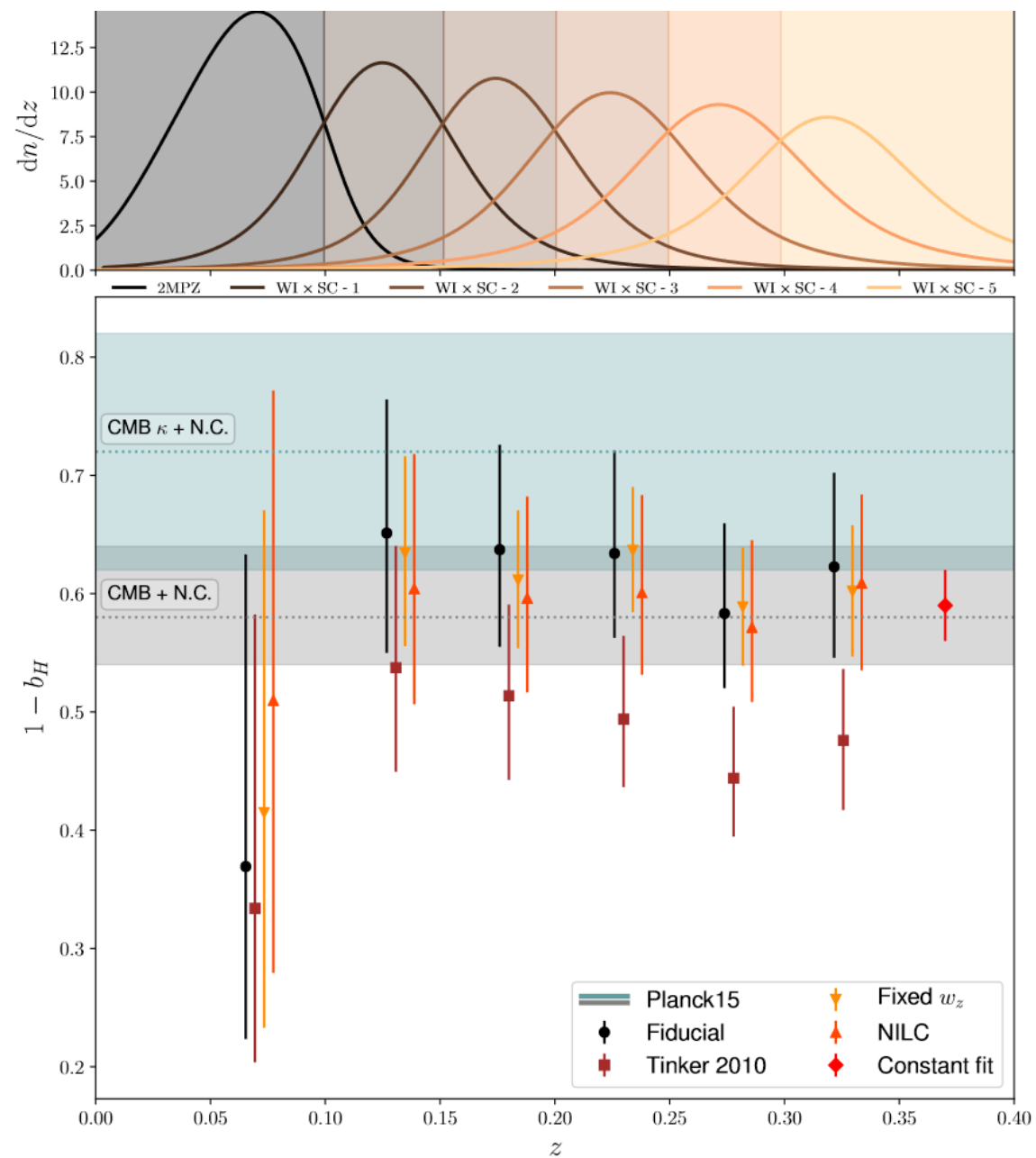
$$T_{uvwz}^{1h} = \int dM \frac{dn}{dM} \langle U(k|M) V(k|M) W(k|M) Z(k|M) \rangle$$

# Fits

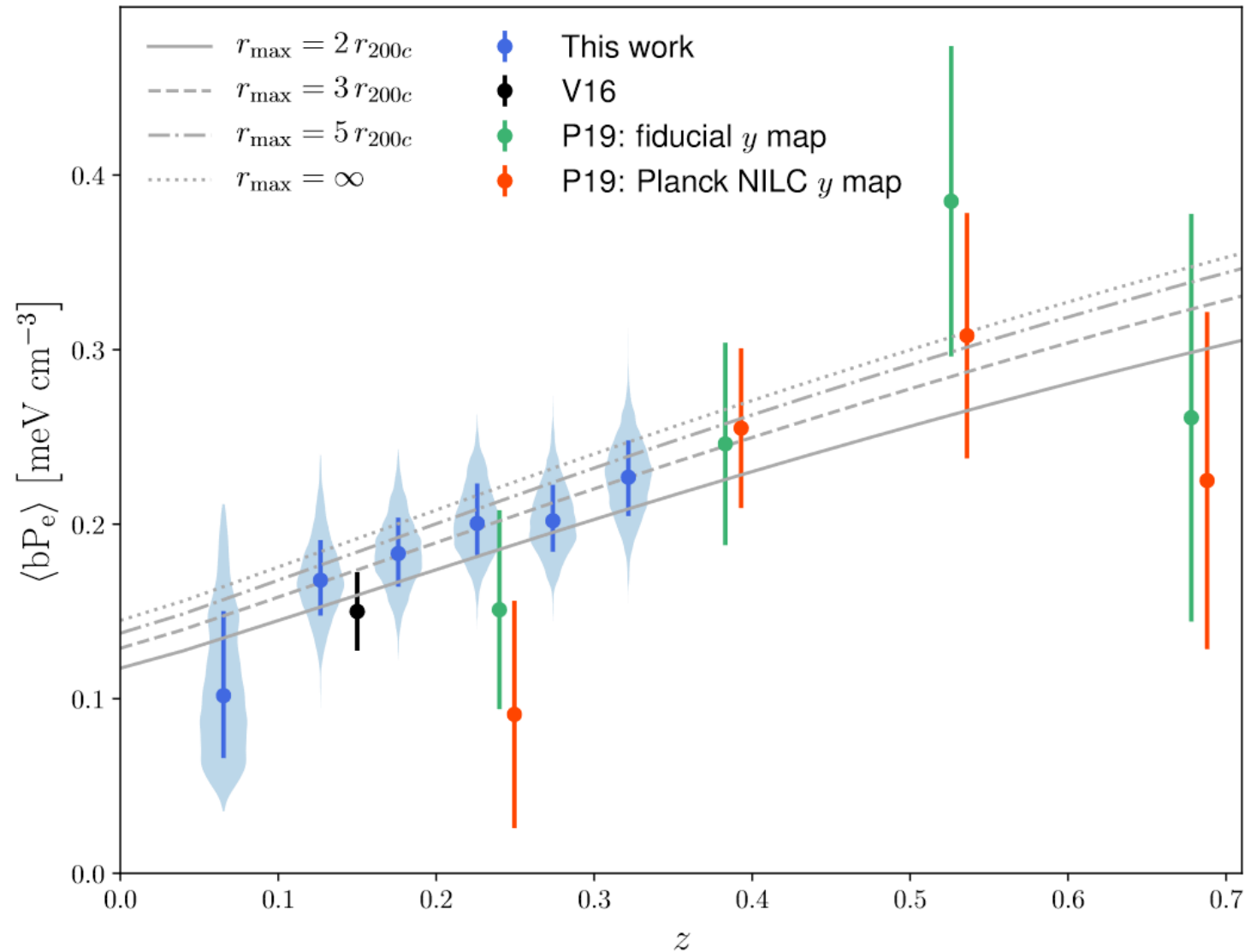
**Data points:** “A unified pseudo- $C_\ell$  framework” (Alonso et al. 2019) - **NaMaster**



# Mass Bias



# Bias-Weighted Thermal Pressure



# Conclusions

# Conclusions

- Cross-correlations to break the degeneracy with  $b_g$ .

# Conclusions

- Cross-correlations to break the degeneracy with  $b_g$ .
- Tomographic measurement of  $(1 - b_H)$ . Agreement with values from Planck clusters and CMB lensing mass calibration. No evidence for redshift dependence.

# Conclusions

- Cross-correlations to break the degeneracy with  $b_g$ .
- Tomographic measurement of  $(1 - b_H)$ . Agreement with values from Planck clusters and CMB lensing mass calibration. No evidence for redshift dependence.
- Planck cosmology used; strongly degenerate with  $\sigma_8$ , but redshift evolution and  $\langle bP_e \rangle$  constraints can only be achieved via tomography.

# Conclusions

- Cross-correlations to break the degeneracy with  $b_g$ .
- Tomographic measurement of  $(1 - b_H)$ . Agreement with values from Planck clusters and CMB lensing mass calibration. No evidence for redshift dependence.
- Planck cosmology used; strongly degenerate with  $\sigma_8$ , but redshift evolution and  $\langle bP_e \rangle$  constraints can only be achieved via tomography.
- Tomographic measurement of  $\langle bP_e \rangle$ . In good agreement with previous results and theory. Best constraints to date.

# Conclusions

- Cross-correlations to break the degeneracy with  $b_g$ .
- Tomographic measurement of  $(1 - b_H)$ . Agreement with values from Planck clusters and CMB lensing mass calibration. No evidence for redshift dependence.
- Planck cosmology used; strongly degenerate with  $\sigma_8$ , but redshift evolution and  $\langle bP_e \rangle$  constraints can only be achieved via tomography.
- Tomographic measurement of  $\langle bP_e \rangle$ . In good agreement with previous results and theory. Best constraints to date.
- Robustness to systematics (CIB, clustering contamination, photo-z).

# Conclusions

- Cross-correlations to break the degeneracy with  $b_g$ .
- Tomographic measurement of  $(1 - b_H)$ . Agreement with values from Planck clusters and CMB lensing mass calibration. No evidence for redshift dependence.
- Planck cosmology used; strongly degenerate with  $\sigma_8$ , but redshift evolution and  $\langle bP_e \rangle$  constraints can only be achieved via tomography.
- Tomographic measurement of  $\langle bP_e \rangle$ . In good agreement with previous results and theory. Best constraints to date.
- Robustness to systematics (CIB, clustering contamination, photo-z).
- Future: ACT, Simons Observatory, Euclid, LSST – higher resolution  $y$ - and CMB lensing- maps, higher redshifts. Better systematics treatment.

# Koukoufilippas, Alonso, Bilicki & Peacock in preparation

the first case is the case of the gas pressure

## Water angle tomographic measurements of the gas pressure through galaxy NGC 4676

V. Koukoufilippas, J. Alonso, M. Bilicki, J. Peacock

Department of Physics, University of Cambridge, Cambridge CB3 0ET, UK  
\* Institute for Astronomy, University of Cambridge, Madingley Road, Cambridge CB3 0ET, UK

ABSTRACT

The water angle tomographic measurements of the gas pressure in the galaxy NGC 4676 are presented. The data are obtained from the  $\text{H}_2\text{O}$  emission lines in the rest-frame of the galaxy. The measurements are performed using the water angle tomographic technique. The results show that the gas pressure is higher in the central region of the galaxy. The measurements are compared with the predictions of the gas pressure profiles. The results are consistent with the predictions of the gas pressure profiles. The measurements are performed using the water angle tomographic technique. The results show that the gas pressure is higher in the central region of the galaxy. The measurements are compared with the predictions of the gas pressure profiles. The results are consistent with the predictions of the gas pressure profiles.

Key words: galaxies: individual (NGC 4676); galaxies: kinematics and dynamics; galaxies: structure

1 INTRODUCTION

The gas pressure in galaxies is a key parameter in understanding the physical processes that govern the evolution of galaxies. The gas pressure is determined by the balance between the inward force of gravity and the outward force of gas pressure. The gas pressure is a key parameter in understanding the physical processes that govern the evolution of galaxies. The gas pressure is determined by the balance between the inward force of gravity and the outward force of gas pressure. The gas pressure is a key parameter in understanding the physical processes that govern the evolution of galaxies. The gas pressure is determined by the balance between the inward force of gravity and the outward force of gas pressure.

© 2015 RAS

The gas pressure in galaxies is a key parameter in understanding the physical processes that govern the evolution of galaxies. The gas pressure is determined by the balance between the inward force of gravity and the outward force of gas pressure. The gas pressure is a key parameter in understanding the physical processes that govern the evolution of galaxies. The gas pressure is determined by the balance between the inward force of gravity and the outward force of gas pressure. The gas pressure is a key parameter in understanding the physical processes that govern the evolution of galaxies. The gas pressure is determined by the balance between the inward force of gravity and the outward force of gas pressure.

© 2015 RAS



Koukoufilippas, Alonso, Bilicki & Peacock  
in preparation  
on the arXiv  
soon.

The first three panels show the gas pressure profiles at three different radii: 10 kpc, 20 kpc, and 30 kpc. The profiles are shown in units of  $10^{-11}$  dyn/cm<sup>2</sup> versus radius in kpc. The profiles show a clear peak at the center, which decreases with radius. The profiles are shown for three different values of the gas pressure profile slope: 0.5, 1.0, and 1.5.

### Wide angle tomographic reconstruction of the gas pressure through galaxy 3D: cross-correlations

Y. F. Koukoufilippas, J. Alonso, M. Bilicki, J. Peacock  
MNRAS, 000, 1-15 (2018)  
https://doi.org/10.1093/mnras/sty1234

ABSTRACT

We use a wide angle tomographic reconstruction of the gas pressure profiles at three different radii: 10 kpc, 20 kpc, and 30 kpc. The profiles are shown in units of  $10^{-11}$  dyn/cm<sup>2</sup> versus radius in kpc. The profiles show a clear peak at the center, which decreases with radius. The profiles are shown for three different values of the gas pressure profile slope: 0.5, 1.0, and 1.5. The profiles are shown for three different values of the gas pressure profile slope: 0.5, 1.0, and 1.5. The profiles are shown for three different values of the gas pressure profile slope: 0.5, 1.0, and 1.5.

1 INTRODUCTION

The gas pressure profiles are shown in units of  $10^{-11}$  dyn/cm<sup>2</sup> versus radius in kpc. The profiles show a clear peak at the center, which decreases with radius. The profiles are shown for three different values of the gas pressure profile slope: 0.5, 1.0, and 1.5. The profiles are shown for three different values of the gas pressure profile slope: 0.5, 1.0, and 1.5. The profiles are shown for three different values of the gas pressure profile slope: 0.5, 1.0, and 1.5.

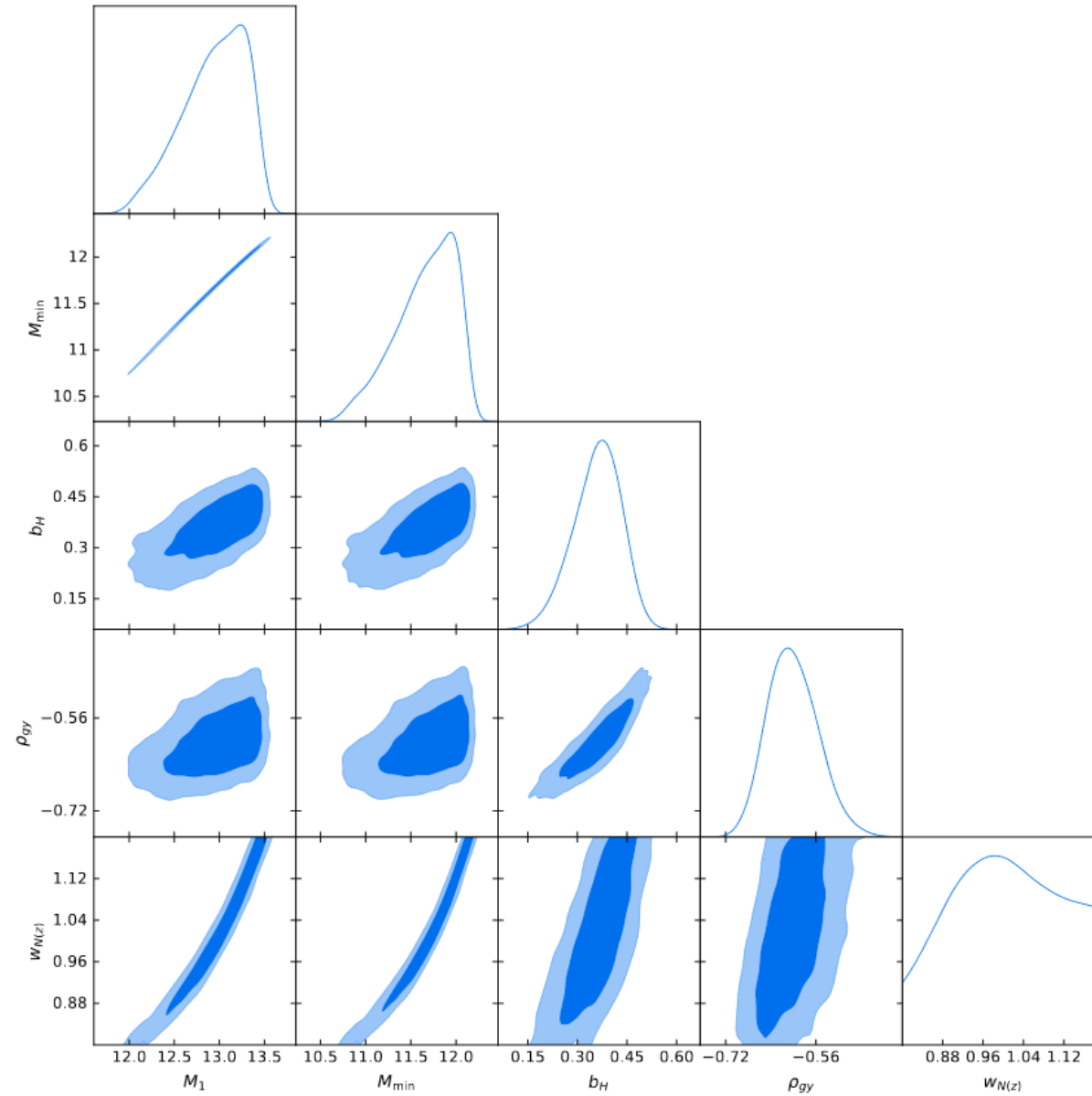
The gas pressure profiles are shown in units of  $10^{-11}$  dyn/cm<sup>2</sup> versus radius in kpc. The profiles show a clear peak at the center, which decreases with radius. The profiles are shown for three different values of the gas pressure profile slope: 0.5, 1.0, and 1.5. The profiles are shown for three different values of the gas pressure profile slope: 0.5, 1.0, and 1.5. The profiles are shown for three different values of the gas pressure profile slope: 0.5, 1.0, and 1.5.

© 0000

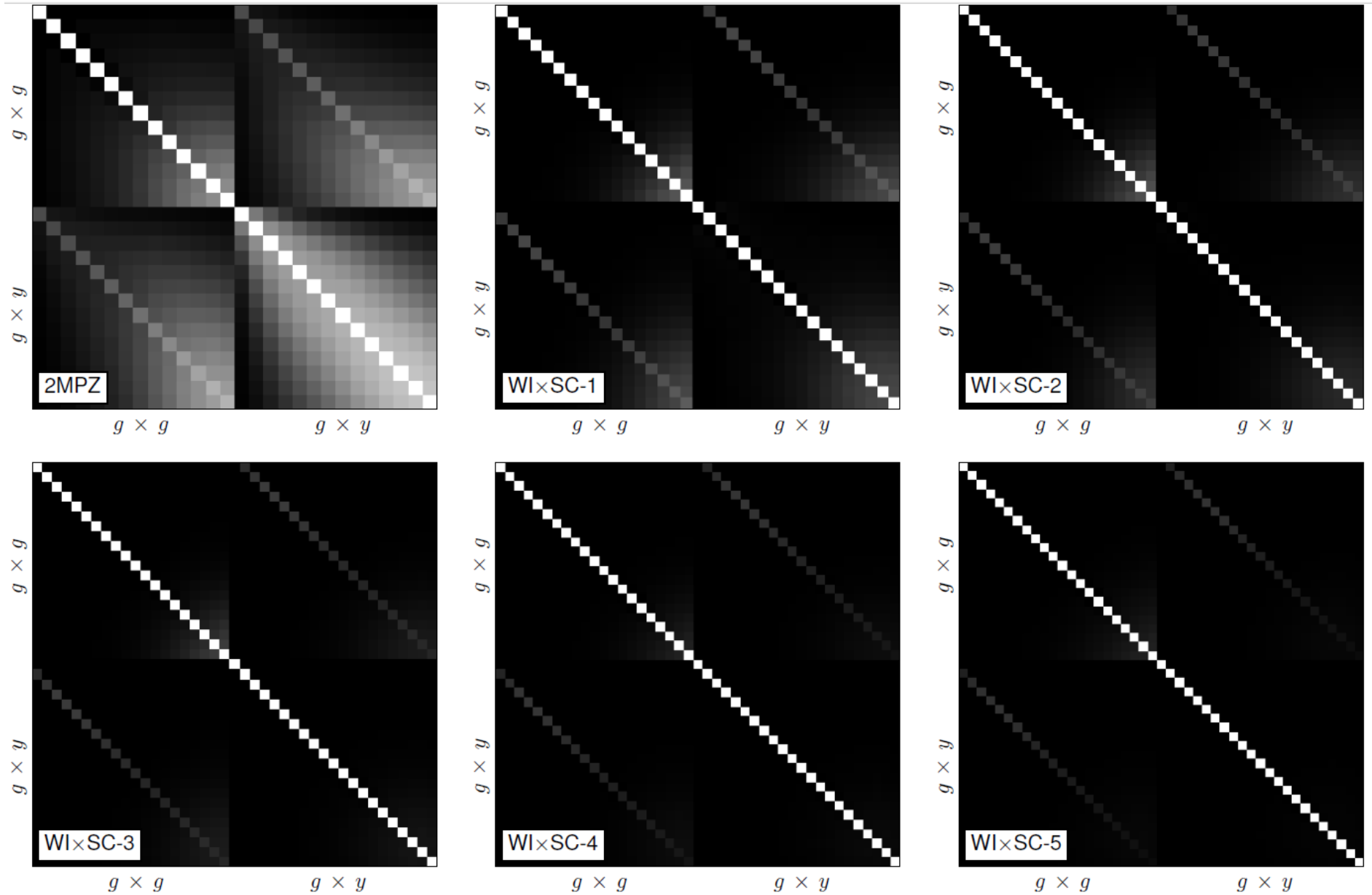


TOMOGRAPHIC MEASUREMENT OF THE COSMIC GAS PRESSURE

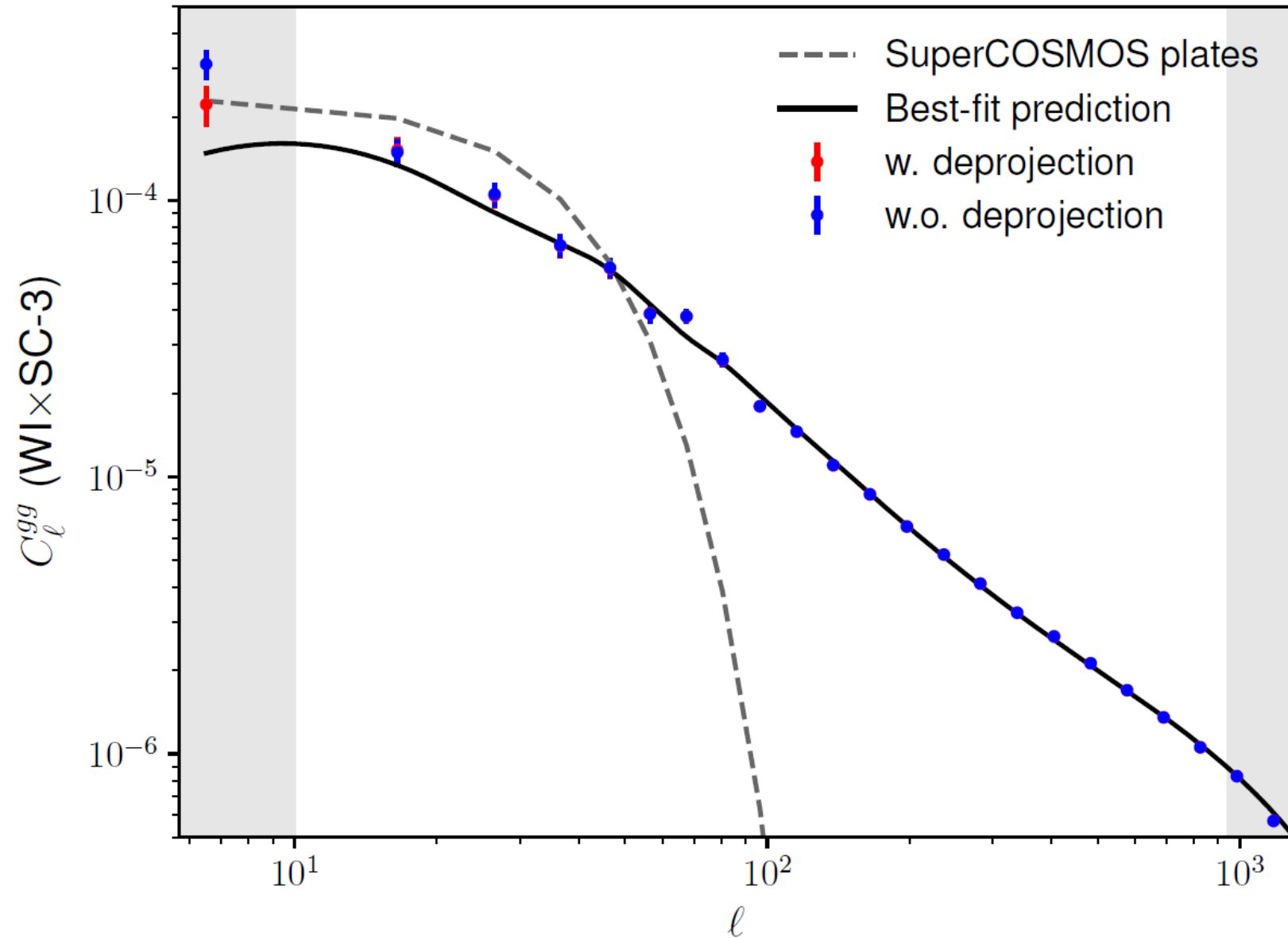
# Parameter space



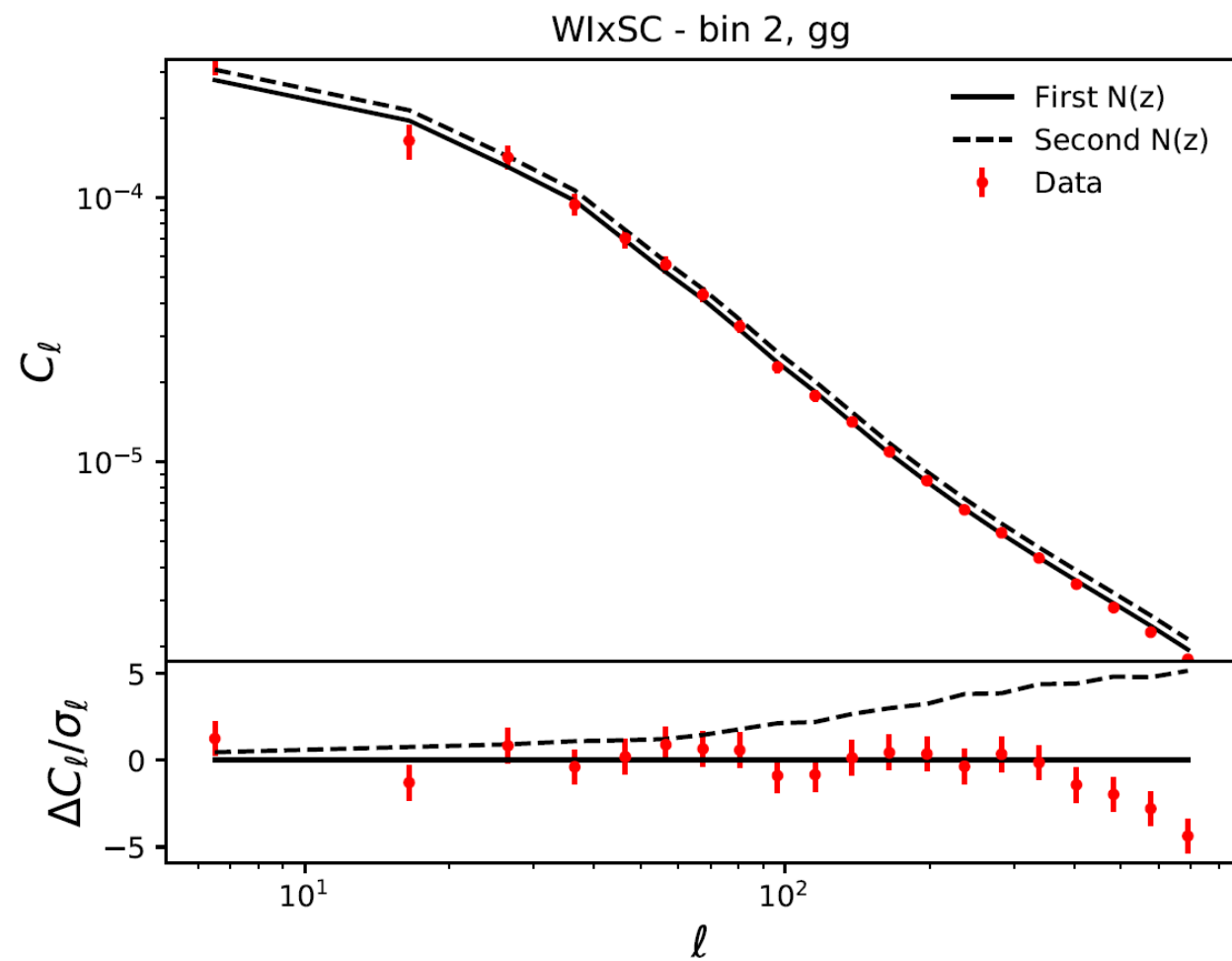
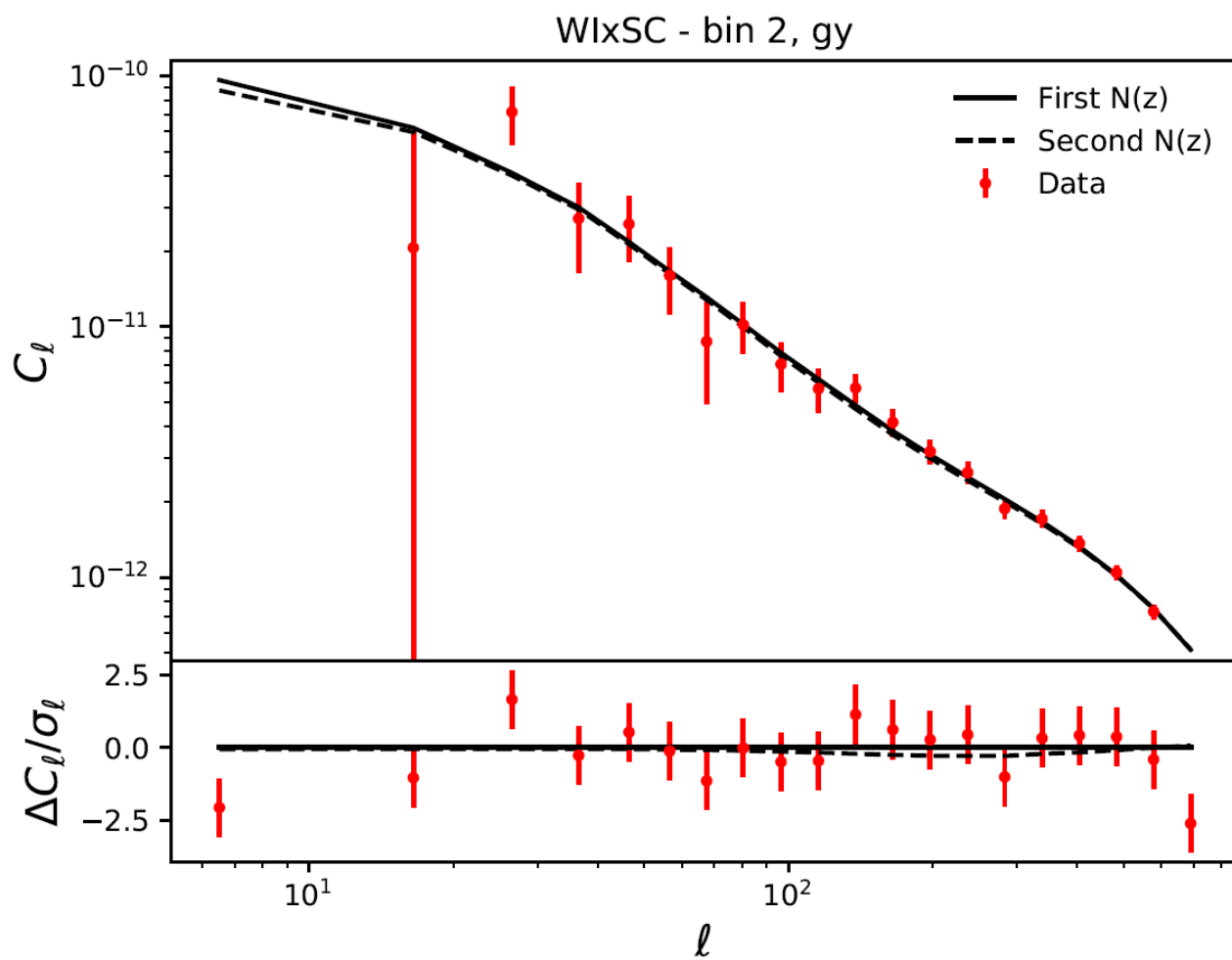
# Correlation matrices



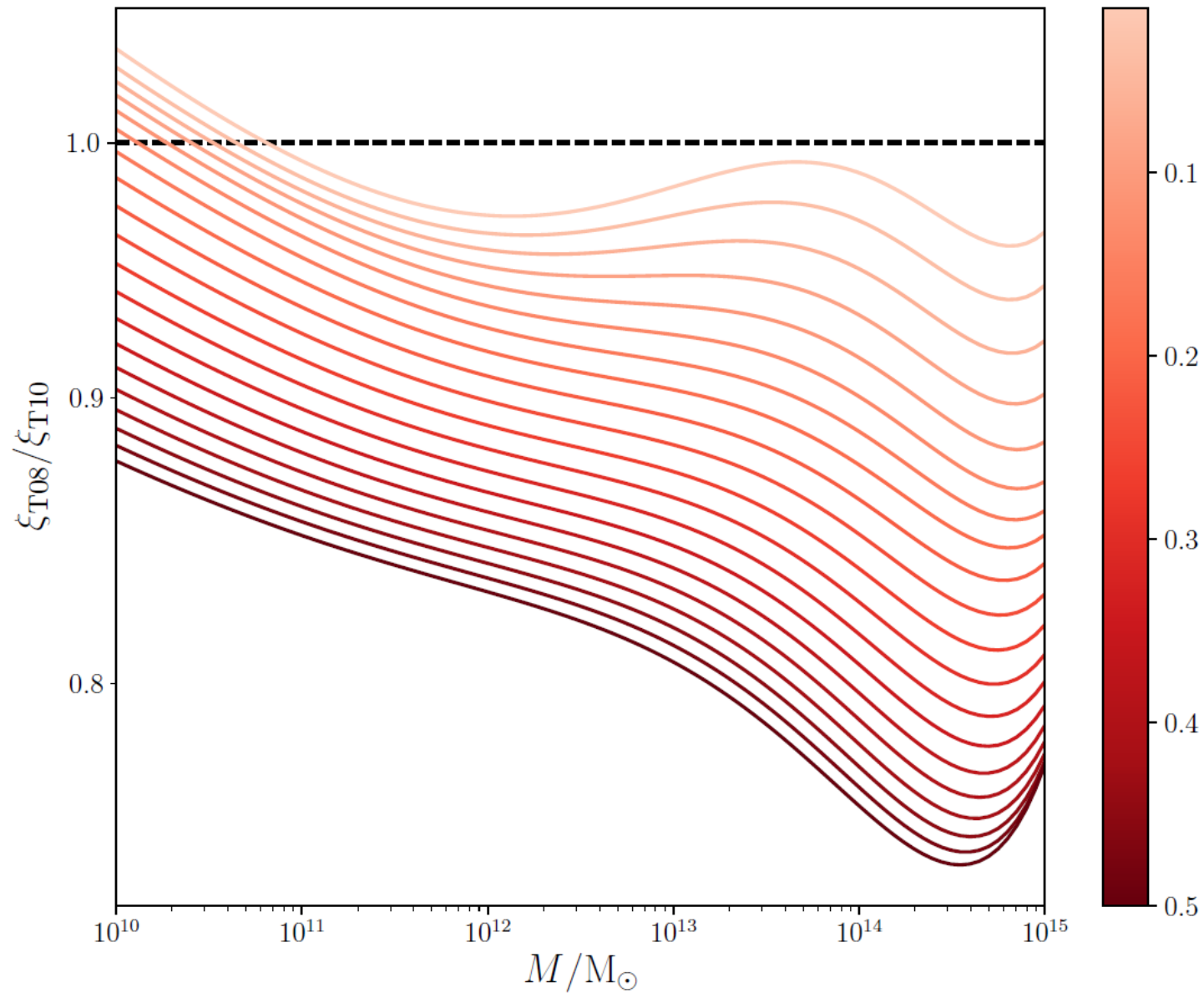
# Systematics analysis



# $w_z$ motivation



# Cosmological mass functions



## Data

